Chemical Geology 531 (2020) 119330

Contents lists available at ScienceDirect

Chemical Geology

journal homepage: www.elsevier.com/locate/chemgeo

# Manganese and cobalt redox cycling in laterites; Biogeochemical and bioprocessing implications

Laura Newsome*, Agustín Solano Arguedas, Victoria S. Coker, Christopher Boothman, Jonathan R. Lloyd

*Williamson Research Centre, School of Earth and Environmental Sciences, University of Manchester, Manchester, M13 9PL, United Kingdom*

ARTICLE INFO

Editor: Hailiang Dong

*Keywords:*
Biogeochemistry
Bioreduction
Cobalt
Nickel
Iron-reduction
Manganese-reduction

ABSTRACT

Cobalt is essential for the modern technology that underpins the decarbonisation of our economies, but its supply is limited leading to its designation as a critical metal. Cobalt biogeochemistry is poorly understood, yet knowledge of how biogeochemical cycling impacts cobalt behaviour could assist the development of new techniques to recover cobalt from ores, and so improve the security of supply. Laterites are an important source of cobalt, they are primarily processed for nickel using energy or chemical intensive processes, with cobalt recovered as a by-product. Metal-reducing conditions were stimulated in laterite sediment microcosms by the addition of simple and cheaply available organic substrates (acetate or glucose). At the end of the experiment the amount of easily recoverable cobalt (aqueous or extractable with acetic acid) increased from < 1% to up to 64%, which closely mirrored the behaviour of manganese, while only a small proportion of iron was transformed into an easily recoverable phase. Sequencing of the microbial community showed that the addition of organic substrates stimulated the growth of indigenous prokaryotes closely related to known manganese(IV)/iron(III)-reducers, particularly from the Clostridiales, and that fungi assigned to *Penicillium,* known to produce organic acids beneficial for leaching cobalt and nickel from laterites, were identified. Overall, the results indicate that the environmental behaviour of cobalt in laterites is likely to be controlled by manganese biogeochemical cycling by microorganisms. These results are compelling given that similar behaviour was observed in four laterites (Acoje, Çaldağ, Piauí and Shevchenko) from different continents. A new bioprocessing strategy is proposed whereby laterites are treated with an organic substrate to generate metal-reducing conditions, then rinsed with acetic acid to remove the cobalt. Not only are organic substrates environmentally-friendly and potentially sourced from waste carbon substrates, a minimal amount of iron oxides was mobilised and consequently less waste generated.

## 1. Introduction

Cobalt is a critical metal essential for a sustainable modern world. It is increasingly in demand for use in rechargeable batteries for solar power and electric cars, permanent magnets in wind turbines, as well as in core applications such as superalloys to increase the strength and resistance of materials, electronics, catalysts, pigments and healthcare (The Cobalt Institute, 2019). Although Co is not rare in the Earth's crust, it is only found in economic quantities in a few countries, with 50 % of reserves in the Democratic Republic of Congo (US Geological Survey, 2018). This has led to Co being designated a critical raw material by the EU in 2011, to highlight the importance of securing a reliable and sustainable supply (European Commission, 2011).

Laterites are an important source of cobalt; they are estimated to comprise 36 % of terrestrial Co deposits (Slack et al., 2017). They are primarily mined for Ni and supply 40 % of the world's annual production (Yongue-Fouateu et al., 2006). Co is recovered as a side product and Ni-laterites supplied 48 % of the world's annual Co production in 2007 (British Geological Survey, 2009), although this had decreased to 15 % by 2011 (Slack et al., 2017). Laterites are iron-rich deposits formed during intense long-lasting weathering of ultramafic bedrock in tropical climates, which leads to the enrichment of residual elements such as Ni and Co. The cobalt in laterites is typically associated with Mn-oxide enriched horizons (Elias et al., 1981; Yongue-Fouateu et al., 2006; Dublet et al., 2017), with a similar relationship observed in soil environments (Taylor and McKenzie, 1966; Uren, 2013). Currently Ni and Co are recovered from laterites using pressure acid leaching, heap leaching and/or solvent extraction (British Geological Survey, 2009;

* Corresponding author. Present address: Camborne School of Mines and Environment and Sustainability Institute, University of Exeter, Penryn, Cornwall, TR10 9FE, United Kingdom.
*E-mail address:* l.newsome@exeter.ac.uk (L. Newsome).

https://doi.org/10.1016/j.chemgeo.2019.119330
Received 19 March 2019; Received in revised form 2 October 2019; Accepted 4 October 2019
Available online 23 October 2019

Kursunoglu and Kaya, 2016; Oxley et al., 2016). A number of studies have demonstrated that Co and Ni can be recovered from laterite and sulfide ores by bioleaching, for example by inoculating the ore with acidophilic cultures such as *Acidothiobacillus* spp. (Johnson et al., 2013; Marrero et al., 2015; Chen et al., 2016; Smith et al., 2017), or fungi that generate organic acids (Tzeferis et al., 1994; Valix et al., 2001). Further research into bioleaching technologies, including field application is ongoing as part of the Natural Environment Research Council CoG3 project (http://www.nhm.ac.uk/our-science/our-work/sustainability/cog3-cobalt-project.html).

Over 30 years ago it was discovered that microorganisms are able to reduce Mn(IV) and Fe(III) coupled to the oxidation of organic carbon or hydrogen, and in doing so gain energy for growth (Lovley and Phillips, 1986; Myers and Nealson, 1988). Under near-neutral and alkaline environmental conditions this can solubilise Mn(IV)-oxide and Fe(III)-oxide minerals by forming aqueous Mn(II) and Fe(II). Microbial metal reduction has since been observed in a broad diversity of prokaryotes from many different environments (Lovley et al., 2004). Although microbial Mn(IV)/Fe(III)-reducers have previously been documented in a Cuban laterite (Perez et al., 2013), their potential to liberate Co from oxide minerals during the development of metal-reducing conditions has not been explored.

The biogeochemistry of cobalt in terrestrial environments is surprisingly poorly understood. Cobalt most frequently occurs as Co(II) or Co(III), with Co(II) thermodynamically stable under most environmental conditions encountered in natural waters (Hem, 1985). An exception to this is where Co is associated with Mn-oxides; Mn-oxides are able to oxidise Co(II) to Co(III) which then sorbs to and becomes incorporated into the Mn-oxide crystal lattice (Murray and Dillard, 1979; Tanaka et al., 2013; Simanova and Peña, 2015). Microbes have been shown to reduce Co(III) to Co(II) under carefully controlled laboratory conditions, for example with Co(III) stabilised using a strong ligand such as EDTA (Gorby et al., 1998; Singh et al., 2015). It has been suggested that concomitant reduction of Mn oxides and Co(III) in soils is required to generate Mn(II) and Co(II) ions that are suitable for uptake by plants (Uren, 2013). In a study in which lake sediments were incubated with *Shewanella putrefaciens*, a model Fe(III)-reducing bacterium, Co and Ni were released to the aqueous phase concurrent with the dissolution of reactive Mn minerals (Crowe et al., 2007). Another study subjected rice paddy soils to reduced conditions by degassing with $N_2/CO_2$ and observed that lower Eh values and the imposed biogeochemical conditions increased Co in the aqueous phase (Shaheen et al., 2014). Together these indicate that microbial metal cycling is likely to play an important role in controlling the mobility of Co in the environment.

The aim of this study was to characterise the biogeochemistry of Co in terrestrial sediment systems, and to use this understanding to inform potentially new and sustainable ways to recover Co from laterites. Here we explored the impact of the adding organic electron donors (acetate or glucose) to biostimulate microbial metal reduction, on the fate of Co and Ni, using microcosms containing four different laterites (Acoje, Çaldağ, Piauí, Shevchenko). A multidisciplinary approach was used to dissect the system, including the use of next-generation DNA sequencing to identify key indigenous microorganisms and X-ray absorption spectroscopy to characterise metal speciation. A simple two-step bioprocessing strategy was designed based on stimulating microbial metal reduction to transform Co from a 'reducible' phase extractable by hydroxylamine-hydrochloride to a more labile 'exchangeable' phase that could be extracted using a simple acetic acid wash.

## 2. Materials and methods

### 2.1. Sample characterisation and experimental set up

#### 2.1.1. Laterite characterisation

Three laterite samples were obtained from the collection of the Natural History Museum, London. These included an actively forming laterite "Acoje" from the Philippines and two laterites that are not currently subject to tropical weathering, "Çaldağ" from Turkey and "Shevchenko 11" from Kazakhstan. Samples were also collected from another laterite not currently subject to tropical weathering in April 2016; the Piauí deposit, Brazil. Two samples were used in these experiments "Piauí 23" and "Piauí 4". All were composite samples collected from heaps and represent a range of horizons throughout the deposits.

Samples of each laterite were dried overnight at 105 °C, powdered in a ball mill and analysed by X-ray diffraction (XRD, Bruker D8 Advance) for mineralogy and X-ray fluorescence (XRF) for chemical composition. Total organic carbon (TOC) measurements were analysed using a Shimadzu SSM5000A. Leach tests were performed by adding 1 g of laterite (wet weight) to 10 ml of deionised water or 30 mM bicarbonate. After 33 days pH measurements were made and the aqueous phase monitored for Co, Fe, Mn and Ni content using inductively coupled plasma atomic emission spectroscopy (ICP-AES, Perkin-Elmer Optima 5300 DV).

#### 2.1.2. Biostimulated Natural History Museum laterite sediment microcosms

Sediment microcosms were set up to investigate whether acetate-biostimulation of indigenous microbial communities in the Natural History Museum (NHM) laterites would generate metal-reducing conditions in the Fe(III) and Mn(IV) containing deposits, and liberate Co and Ni. These contained 3 g of laterite (wet weight), 30 ml of an anaerobic modified freshwater minimal medium (after Lovley et al., 1991) at pH 7 with 10 mM acetate as the electron donor. The headspace was degassed with an 80:20 $N_2$:$CO_2$ mix and the bottles incubated in the dark at 30 °C. Experiments were conducted in triplicate and compared to no added electron donor controls.

#### 2.1.3. Bioaugmented Natural History Museum laterite sediment microcosms

Parallel NHM laterite sediment microcosms were augmented with a model Fe(III)-reducing bacterium (*Geobacter sulfurreducens*) to generate strongly Fe(III)-reducing conditions. These comprised 3 g of laterite, 30 ml of 30 mM sodium bicarbonate, 10 mM acetate and a washed cell suspension of *G. sulfurreducens* at an optical density at 600 nm of 0.8. *G. sulfurreducens* was obtained from the University of Manchester Geomicrobiology Laboratory culture collection and grown at 30 °C in the dark in an anaerobic modified freshwater enrichment medium (after Lovley and Phillips, 1988) at pH 7, with 15 mM acetate as the electron donor and 40 mM fumarate as the electron acceptor. Cells were harvested at the late-logarithmic phase by centrifugation (5000 *g*, 20 min), washed twice in anaerobic 30 mM bicarbonate buffer, before adding to the sediment microcosms. Experiments were conducted in triplicate and compared to no added electron donor controls.

#### 2.1.4. Biostimulated Piauí laterite sediment microcosms

To test the ability of different electron donors to stimulate metal-reducing conditions and consequently mobilise Co and Ni, sediment microcosms were set up with the Piauí laterite and biostimulated with two different electron donors. These contained 3 g of laterite, 30 ml of sterile artificial groundwater (Wilkins et al., 2007), and either 5 mM acetate and 5 mM lactate or 10 mM glucose. The headspace was degassed with an 80:20 $N_2$:$CO_2$ mix and the bottles incubated in the dark at 30 °C. Subsequently glucose was selected as the more effective electron donor and the microcosms were repeated with 10 g laterite, 100 ml artificial groundwater and 10 mM glucose in triplicate and compared to no added electron donor controls. As significant heterogeneities were observed, these were repeated with duplicate glucose-biostimulated sediment microcosms and an additional no added electron donor control.

### 2.2. Aqueous geochemistry

Aliquots of sediment slurry were periodically removed from sediment microcosms using a sterile $N_2$ degassed needle and syringe, and monitored for geochemical changes. In brief, 0.1 ml of slurry was added to 4.9 ml 0.5 N HCl or 0.5 N hydroxylamine-hydrochloride and digested for 1 h before analysis for Fe(II) and total bioavailable Fe by the ferrozine assay (Lovley and Phillips, 1986, 1987). Supernatant was obtained by centrifugation (16,200 *g*, 5 min). The supernatant was analysed for major anions and volatile fatty acids using ion chromatography (Dionex ICS 5000). pH and Eh were measured using calibrated electrodes. Glucose concentrations in supernatant from selected samples were monitored using a Glucose Oxidase (GO) Assay Kit (Sigma). An aliquot of the supernatant was diluted into 2 % $HNO_3$ and analysed for Co, Fe, Mn and Ni via ICP-AES.

### 2.3. Microbial community analysis

The prokaryotic and fungal communities were characterised for each of the laterites to identify the composition of the indigenous microbial communities, and the groups that responded to biostimulation. Samples were analysed at the start and the end of the biostimulation experiments, including the microcosms stimulated with electron donor and the no added electron donor controls. For the NHM laterites microbial community characterisation was performed on the Day 0 and Day 90 time points, and on Days 0, 28 and 76 for the Piauí laterite. DNA was extracted from 0.2 ml of sediment slurry using a PowerSoil DNA isolation kit (MO Bio).

#### 2.3.1. Prokaryotic community analysis

The prokaryotic DNA was amplified using the universal 16S rRNA amplicon primers 8 F and 1492R (Lane, 1991) and the purity of the polymerase chain reaction (PCR) products was determined by visualisation under short-wave UV light after staining with Sybersafe® and separation by electrophoresis in Tris-acetate-EDTA gel. The PCR products were cleaned up, quantified and the 16S rRNA genes were sequenced using the Illumina MiSeq platform (Illumina, San Diego, CA, USA) targeting the V4 hyper variable region (forward primer, 515 F, 5′-GTGYCAGCMGCCGCGGTAA-3′; reverse primer, 806R, 5′-GGACTACHVGGGTWTCTAAT-3′) for 2 × 250-bp paired-end sequencing (Illumina) (Caporaso et al., 2011, 2012). PCR amplification was performed using Roche FastStart High Fidelity PCR System (Roche Diagnostics Ltd, Burgess Hill, UK) in 50 μl reactions under the following conditions: initial denaturation at 95 °C for 2 min, followed by 36 cycles of 95 °C for 30 s, 55 °C for 30 s, 72 °C for 1 min, and a final extension step of 5 min at 72 °C. The PCR products were purified and normalised to ~20 ng each using the SequalPrep Normalization Kit (Fisher Scientific, Loughborough, UK). The PCR amplicons from all samples were pooled in equimolar ratios. The run was performed using a 4 pM sample library spiked with 4 pM PhiX to a final concentration of 10 % following the method of Schloss and Kozich (Kozich et al., 2013).

Raw sequences for prokaryotes were divided into samples by barcodes (up to one mismatch was permitted) using a sequencing pipeline. Quality control and trimming was performed using Cutadapt (Martin, 2011), FastQC (https://www.bioinformatics.babraham.ac.uk/projects/fastqc/), and Sickle (Joshi and Fass, 2011). MiSeq error correction was performed using SPADes (Nurk et al., 2013). Forward and reverse reads were incorporated into full-length sequences with Pandaseq (Masella et al., 2012). Chimeras were removed using ChimeraSlayer (Haas et al., 2011), and operational taxonomic units (OTUs) were generated with UPARSE (Edgar, 2013). OTUs were classified by Usearch (Edgar, 2010) at the 97 % similarity level, and singletons were removed. Rarefaction analysis was conducted using the original detected OTUs in Qiime (Caporaso et al., 2010). The taxonomic assignment was performed by the RDP classifier (Wang et al., 2007) and Blastn was used to identify the closest GenBank matches (http://blast.ncbi.nlm.nih.gov).

#### 2.3.2. Fungal community analysis

The fungal DNA was amplified using the Internal Transcribed Spacer Region (ITS) primers ITS1F and ITS4 (Brown et al., 1993; Gardes and Bruns, 1993) and the purity of the polymerase chain reaction (PCR) products was determined by visualisation under short-wave UV light after staining with Sybersafe® and separation by electrophoresis in Tris-acetate-EDTA gel. Sequencing of PCR amplicons of the ITS2 region of nuclear ribosomal DNA was conducted with the Illumina MiSeq platform (Illumina, San Diego, CA, USA), targeting the ITS2 internal transcribed spacer region between the large subunit (LSU) and the 5.8S ribosomal genes (forward primer, ITS4F, 5′- AGCCTCCGCTTATTGATATGCTTAART -3′, reverse primer, 5.8SR, 5′- AACTTTYRRCAAYGGATCWCT -3′;) (Taylor et al., 2016) for 2 × 300-bp paired-end sequencing (Illumina) (Caporaso et al., 2011, 2012). PCR amplification was performed using Roche FastStart High Fidelity PCR System (Roche Diagnostics Ltd, Burgess Hill, UK) in 50 μl reactions under the following conditions: initial denaturation at 95 °C for 2 min, followed by 36 cycles of 95 °C for 30 s, 56 °C for 45 s, 72 °C for 2 min, and a final extension step of 5 min at 72 °C. The PCR products were purified and normalised to ~20 ng each using the SequalPrep Normalization Kit (Fisher Scientific, Loughborough, UK). The PCR amplicons from all samples were pooled in equimolar ratios. The run was performed using a 10 pM sample library spiked with 10 pM PhiX to a final concentration of 10 % following the method of Schloss and Kozich (Kozich et al., 2013).

The ITS sequencing data produced by the Miseq platform was analysed using the PIPITS automated pipeline (Gweon et al., 2015). Chimeras were removed by reference based chimera detection using UCHIME (Edgar et al., 2011) in conjunction with the UNITE UCHIME reference data set. The taxonomic assignment was performed by the RDP classifier (Wang et al., 2007) using the UNITE fungal ITS reference data set.

#### 2.3.3. Microbial community abundances

The abundance of prokaryotic DNA was determined in selected samples using quantitative PCR (qPCR). A serial dilution series was performed using a gBlock double stranded DNA gene fragment (Integrated DNA Technologies, Leuven, Belgium) covering nucleotide positions 1–570 of the 16S rRNA gene from species *Telluria mixta DSM 4832*. The standard curve for the qPCR reaction was created by plotting the $C_T$ (Cycle threshold) values of the dilution series against the log input of DNA template. Concentrations ranging from $8.4 \times 10^{-2}$ fg $\mu l^{-1}$ to $8.4 \times 10^{5}$ fg $\mu l^{-1}$ were used to generate the standard curve.

PCR amplification was performed using Brilliant II SYBR Green QPCR Master Mix (Agilent Technologies LDA UK Limited, Stockport, UK) in a 25 μl final volume containing 2 μl of sample DNA, 0.15 μM of each primer and 12.5 μl of qPCR SYBR Green Master Mix. All the amplifications were carried out in optical grade qPCR tubes on a MX3000 P qPCR system with an initial step of 94 °C for 10 min followed by 30 cycles of 94 °C for 30 s, 50 °C for 30 s, 72 °C for 45 s and a dissociation curve was run between 94 °C and 50 °C to check primer specificity. Cycle threshold ($C_T$) was determined automatically by the instrument. All samples were analysed in triplicate and the $r^2$ value was 0.986.

### 2.4. Solid geochemistry and mineralogy

#### 2.4.1. Sequential extractions

The distribution of metals in the laterites before and after biostimulation (with the added carbon substrates) and bioaugmentation (with added cells of *G. sulfurreducens*) was assessed using sequential extractions, allowing changes in metal extractability to be determined. The modified BCR procedure was used (Rauret et al., 1999; Bacon and Davidson, 2008) with 0.5 g of dried sediment and comprised extraction steps of 0.11 M acetic acid for the “exchangeable” fraction, 0.5 M hydroxylamine hydrochloride for the “reducible” fraction, 8.8 M hydrogen peroxide and 1.0 M ammonium acetate for the “oxidisable”

fraction, and aqua regia for the "residual" fraction. For the biostimulated sediment the first two steps were done under anaerobic conditions to avoid mobilisation by oxidation (Keith-Roach et al., 2003). Extracts were analysed for Co, Mn, Fe and Ni using ICP-AES.

#### 2.4.2. Mineralogy of microbially-reduced laterite sediment

At the end of the experiments (33 days for the bioaugmented NHM sediment microcosms, 90 days for the acetate-biostimulated NHM laterite microcosms, 143 days for the glucose-biostimulated Piauí microcosms) the solid phase was separated from the aqueous phase by centrifugation (5000 *g*, 20 min), the resulting sediment paste was dried anaerobically, and powdered by hand in an anaerobic cabinet using a pestle and mortar. XRD (Bruker D8 Advance) was performed on the dried sediment using a Coy anaerobic dome to assess for changes in mineralogy.

#### 2.4.3. Metal speciation by XAS

To investigate changes in metal speciation, iron and nickel $L_{II}$ and $L_{III}$ edge X-ray absorption spectroscopy (XAS) in conjunction with X-ray magnetic circular dichroism (XMCD) was carried out on the laterites before and after biostimulation using the 6.3.1 beamline at the Advanced Light Source, Berkeley, CA which has an energy range of 250–2000 eV, a spot size of 180 μm x 80 μm and utilises a variable-line-spacing plane-grating (VLS-PGM). Measurements were made on dry samples prepared and analysed under anaerobic conditions, using total electron yield (TEY) to achieve an effective probing depth of around 3–4 nm on samples orientated perpendicular to the beam. Two XAS spectra were collected using opposing applied magnetic fields of ± 1 T parallel and antiparallel to the beam direction, normalised to the incident beam and subtracted from each other to give XMCD spectra (Pattrick et al., 2002; Coker et al., 2008); three pairs of spectra were collected and averaged. It was not possible to obtain *L*-edge spectra for Co and Mn on these beamlines due to the low concentrations of these elements in the laterites. *L*-edge XAS spectra were compared qualitatively to known standards for goethite, ferrihydrite and magnetite (Joshi et al., 2018) as well as a calculated spectrum for $Ni^{2+}$ in octahedral coordination (van der and Kirkman, 1992; Coker et al., 2008).

High resolution X-ray absorption near edge spectra (HR-XANES) were obtained for the Co and Ni *K*-edges using the I20 beamline at the Diamond Light Source. *K*-edge EXAFS spectra were also obtained for Ni but Co concentrations were too low for EXAFS analyses. The I20 beamline has an energy range of 4–20 keV and uses a four bounce monochromator with Si(111) crystals (Hayama et al., 2018), a 64 element fluorescence Ge detector, and for these experiments Al foil was used to reduce contributions from Fe. All samples were measured at room temperature. HR-XANES measurements were made using X-ray Emission Spectroscopy (XES), comprising a 1 m Rowland circle spectrometer and three Si(531) analyzer crystals to fully separate the Fe Kβ and Co Kα fluorescence lines. Four HR-XANES scans were performed on each sample, with no significant changes observed in scans over time, indicating that neither beam damage nor photo-reduction occurred during analysis. The detection limit for Co XANES was not determined, but measurements were limited to around 1000 mg $kg^{-1}$ for Co *K*-edge EXAFS due to the geometry of the spectrometer. Ni EXAFS measurements were made using the 64 element Ge detector. Between four and six scans were made per sample. The detection limits depend on the sample matrix, but are estimated to be around 50 mg $kg^{-1}$ for Ni *K*-edge EXAFS. ATHENA (Ravel and Newville, 2005) was used to calibrate, background subtract and normalise XANES spectra, and to remove glitches in the data at around 8620, 8928 and 9013 eV. ARTEMIS (Ravel and Newville, 2005) was used to fit the Ni EXAFS spectra, with additional shells only included if they significantly improved the fitting parameters (Downward et al., 2007).

**Table 1**
Metal content of the laterites (dry weight, %).

| Composition by XRF (%) | Çaldağ | Acoje | Shevchenko 11 | Piauí 4 | Piauí 23 |
|---|---|---|---|---|---|
| Mn | 0.32 | 0.64 | 0.91 | 0.22 | 0.38 |
| Fe | 30.6 | 44.6 | 20.5 | 13.4 | 24.7 |
| Co | 0.05 | 0.05 | 0.13 | 0.03 | 0.07 |
| Ni | 0.14 | 0.16 | 0.17 | 0.27 | 0.21 |

## 3. Results and discussion

### 3.1. Laterite characterisation

Each laterite contained the common rock forming minerals quartz and Al and/or Mg silicates (such as clinochlore, antigorite, lizardite, talc), as well as the Fe(III)-oxide goethite (Table S1). The Acoje laterite contained the mixed Fe(II)/Fe(III) minerals maghemite and hornblende, which together with the higher water content may indicate a lower degree of weathering, and potentially reflect that this laterite is actively forming. The Mn, Fe, Co and Ni contents of the laterites are listed in Table 1, correlation plots showed Mn and Co were positively correlated, and a negative correlation between Fe and Si (Fig. S1). The concentrations of Mn and Co measured were within the range of those reported for the Lomié laterite, Cameroon (Yongue-Fouateu et al., 2006), the New Caledonia laterite (Dublet et al., 2017), the Brolga deposit, Australia and the Bonsora Sorako deposit, Indonesia (Marsh et al., 2013). Metals in all four laterites were mostly insoluble; less than 0.01 mM Co, Mn and Ni, and less than 0.1 mM of Fe were released to solution from leaching of the laterites with deionised water or 30 mM bicarbonate (except for Piauí 4 which released 0.09 ± 0.01 mM Ni to solution after 33 days in deionised water) (Table S1). The pH of the laterites in deionised water ranged from 6.3 to 8.7, TOC was between 0.05 and 0.23 % and the water were: Çaldağ 6.8 %, Acoje 26 %, Shevchenko 11 6.5 %, Piauí 4 28 % and Piauí 23 13 % (Table S1).

### 3.2. Natural History Museum laterite microcosms

Samples of the Acoje, Çaldağ and Shevchenko laterites were biostimulated with acetate or bioaugmented with *Geobacter sulfurreducens* and acetate to stimulate the development of metal-reducing conditions, observe the impact on Co and Ni extractability, and to identify the indigenous prokaryotes likely responsible.

#### 3.2.1. Stimulated microbial metal reduction in the NHM laterite sediment microcosms

Aqueous geochemical monitoring showed that Fe(III)-reducing conditions rapidly developed in each of the microcosms augmented with *G. sulfurreducens* (results are shown in Fig. 1 for the Acoje laterite, and for brevity the Çaldağ and Shevchenko laterites are in the supporting information respectively as Fig. S2 and S3). After just 24 h of incubation, Fe(II) had been produced in the bioaugmented Çaldağ and Shevchenko laterites, while Fe(II) was first measured in the Acoje laterite on Day 7. After 33 days considerable quantities of Fe(II) had been generated in the Çaldağ (62 ± 44 mM) and Acoje (23 ± 8.8 mM) microcosms. The texture of the laterites had changed significantly in the bioaugmented microcosms (Fig. S4), with an absence of a visible finer grained fraction and significant clumping of the sediment meaning it very rapidly settled from solution after shaking. This was particularly pronounced in the Shevchenko laterite which meant it was not possible to obtain a representative sample using a needle and syringe, hence the low Fe(II) concentrations reported with relatively large errors (1.6 ± 0.8 mM). These physical changes were not observed in the no added electron donor controls. The results for each of the biostimulated NHM laterite microcosms were similar, with Fe(II) produced and reducing conditions developed, albeit at a slower rate.

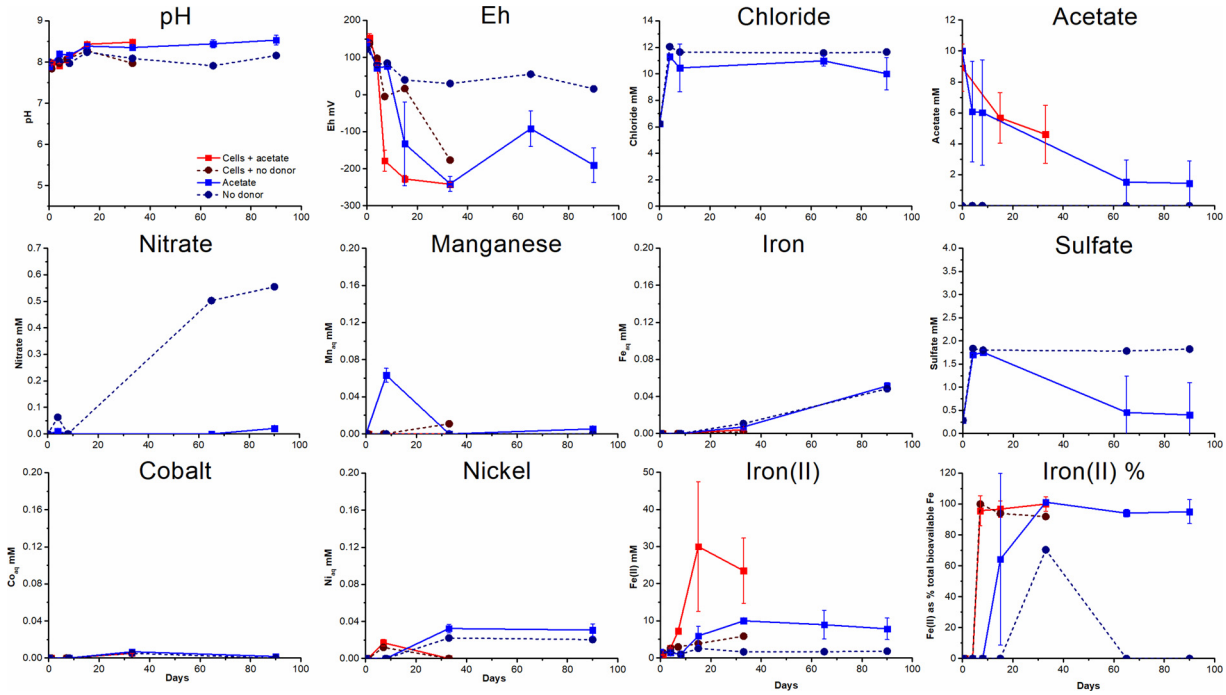


**Fig. 1.** Geochemical monitoring of the biostimulated (blue, monitored to Day 90) and bioaugmented (red, monitored to Day 33) Acoje laterite sediment microcosms. Results are the average of three values; error bars ± 1 standard deviation (SD). ND refers to the single no added electron donor controls (dashed lines). The bioaugmented microcosms were stopped after 33 days. Very low concentrations of metals were released to the aqueous phase; just above the method reporting limit of 0.01 mM. Sediment clumping made it difficult to obtain a representative sample for Fe(II) measurement by the Ferrozine assay, generating relatively large SDs.

Less than 0.1 mM of Fe, Mn, Ni or Co was measured in the aqueous phase in all biostimulated and bioaugmented laterite sediment microcosms (Figs. 1, S2, S3), indicating that any geochemical transformations involving these elements, such as the production of Mn(II) or Fe(II), must have been limited to the solid phase. Anions were monitored in the biostimulated sediment microcosms to investigate the development of reducing conditions; the results showed that acetate was used by the sediment microbial community and small quantities of nitrate and large quantities of sulfate were released to the aqueous phase (Figs. 1, S2, S3). The sulfate concentrations then decreased over time in the Çaldağ and Acoje biostimulated microcosms, presumably by microbial sulfate reduction.

### *3.2.2. Sequential extractions to investigate metal fate in the NHM laterite sediment microcosms*

Sequential extractions were performed to investigate the fate of metals in the solid phase. This included the laterite as supplied, and samples of the sediment microcosms 90 days after biostimulation with acetate, and 33 days after bioaugmentation with *G. sulfurreducens,* together with corresponding no added electron donor controls.

For each laterite, in the sediment as supplied (and the Day 90 no added electron control) most of the Co and Mn were associated with the 0.5 M hydroxylamine-extractable "reducible" phase, and most of the Ni and Fe were associated with the aqua regia-extractable "residual" phase (Figs. 2, S5, S6). In contrast, the biostimulated and bioaugmented laterites showed significantly more Co and Mn (and some Ni) were present in the acetic acid-extractable "exchangeable" phase. Therefore, although these metals were not released to the aqueous phase during microbial metal reduction (Figs. 1, S2, S3), they were instead transformed from a likely crystalline "reducible" phase into a loosely bound "exchangeable" or sorbed phase, and similar behaviour was observed in all three laterites.

The proportion of Co associated with easily recoverable phases in the laterites (that is, the aqueous content plus the acetic-acid extractable "exchangeable" fraction) after biostimulation or bioaugmentation increased from < 1 % to up to 45 % while Ni increased from < 1.5 % to up to 11 % (Table 2). Easily recoverable Mn also increased from < 1.5 % to up to 68 %, likely via microbial Mn(IV) reduction associated with the development of reducing conditions, while easily recoverable Fe increased from 0 % to 4.8 %.

### *3.2.3. Changes to the NHM laterite microbial communities during acetate biostimulation*

The composition of the microbial community in the acetate-biostimulated sediment microcosms and associated no electron donor controls was characterised by Illumina sequencing for prokaryotes (all laterites) and fungi (Acoje laterite). The most frequently detected prokaryotic sequences in the Day 0 microbial communities tended to be from the Acidobacteria, Actinobacteria, Bacteriodetes and Proteobacteria, reflecting typical soil environments (Fig. 3). The abundance of 16S rRNA genes detected in the laterites at Day 0 was low (4.5 – 9.3 fg $g^{-1}$ laterite) (Table S2) and considerably lower than values previously reported from Cuban laterites (Perez et al., 2013); reported in copy number per gram dry sample were in the order of $1 \times 10^7$ - $1 \times 10^8$, compared to $1.1 \times 10^4$ – $2.2 \times 10^4$ here.

After 90 days incubation the diversity of the prokaryotic communities had decreased slightly in most microcosms, and was substantially lower in the acetate-amended Acoje and Shevchenko sediments (Table S2), perhaps reflecting their becoming dominated by relatively few OTUs (Table S2). Compared to the Day 0 results the number of OTUs was higher after 90 days incubation in the Acoje and Çaldağ samples, but similar in the Shevchenko sample, with similar trends observed for the acetate-amended samples and no electron donor controls (Fig. S7). The abundance of 16S rRNA genes was quantified for the Acoje laterite and increased over 90 days in both the acetate amended microcosms (from 9.3–384 fg $g^{-1}$) and the no electron donor control (from 4.5–155 fg $g^{-1}$) (Table S2). This indicates that incubation of the sediment microcosms either enhanced prokaryotic growth regardless of electron donor addition, or broke down the laterite substrate to make it more amenable to DNA extraction. Over the course of the experiment

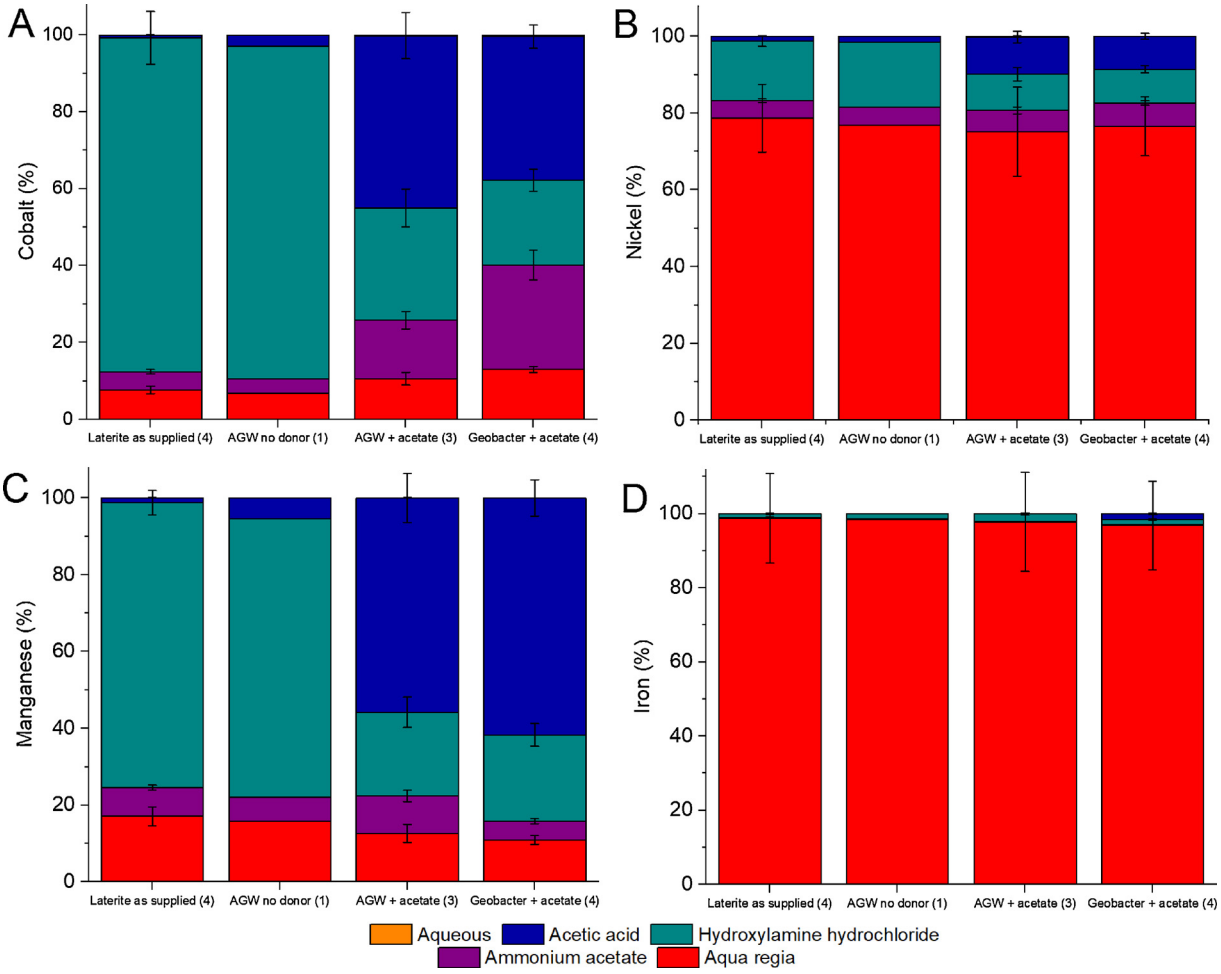


**Fig. 2.** Analysis of metal distribution in the Acoje laterite using sequential extractions (A) cobalt (B) nickel (C) manganese (D) iron. The laterites as supplied and the no electron donor control (left hand columns) showed very little metals in the acetic-acid extractable "exchangeable" phase. Biostimulation and bioaugmentation (right hand columns) increased the proportion of Co, Mn and Ni associated with the "exchangeable" phase. Numbers in brackets represent the replicates used for the sequential extraction procedure.

the OTUs that had dominated the Day 0 samples had decreased substantially, in most cases to comprise less than 1 % of the corresponding Day 90 samples for both the acetate-amended microcosms and no electron donor controls. This demonstrates that incubation in sediment microcosms has a significant effect on microbial community composition, which therefore needs to be taken into account when observing the impact of biostimulation by comparing the results against changes in the no electron donor controls (Table S3).

Acetate biostimulation of laterite sediment microcosms caused the Day 90 microbial communities to become dominated by Firmicutes, Betaproteobacteria and Deltaproteobacteria (Figs. 3A–C, S9, Table S3). The proportion of sequences closely related to known Mn(IV)/Fe(III)-reducers increased in each laterite (Fig. S8). The most frequently detected OTUs in the acetate-amended Acoje and Çaldağ laterites were from the Clostridiales, many of which are obligate anaerobes and spore formers (Vos et al., 2009); sequences assigned to the *Thermincola* genus and most closely related to uncultured bacteria from acetate biostimulation and Fe(III)-reducing environments comprised 40 % of the Acoje and 28 % of the Çaldağ prokaryotic communities. Other notable Fe(III)-reducers included sequences most closely related to *Geosporobacter subterraneus* (also from the Clostridiales) which comprised 10 % of the Shevchenko community, and sequences assigned to the *Anaeromyxobacter* genus which comprised 10 % of the Çaldağ and 26 % of the Shevchenko communities.

Sulfate-reducing *Desulfurispora* formed 10 % of the Day 90 Çaldağ prokaryotic community, reflecting the geochemical data which showed that sulfate reduction occurred in this sample (Fig. S2). Sulfate reduction also occurred in the Acoje microcosms (Fig. 1) but not in the Shevchenko microcosms (Fig. S3). In both the Çaldağ and Acoje samples the proportion of sequences assigned to the *Thermincola* genus increased substantially over the course of the experiment. *Thermincola* spp. have been shown to reduce thiosulfate but not sulfate (Zavarzina et al., 2007). The Day 90 Shevchenko prokaryotic community was dominated by sequences most closely related to *Azoarcus anaerobius (*48 %), a strict anaerobe that can respire nitrate (Reinhold-Hurek and Hurek, 2006). OTUs most closely related to the aforementioned Clostridiales groups, *Anaeromyxobacter, Desulfurispora, Thermincola* and *Azoarcus* spp. comprised less than 0.1 % of the Day 90 no added electron donor controls (Table S3), suggesting that their growth was stimulated by the addition of acetate, and that they likely contributed to the reduction of terminal electron acceptors in the laterite sediment microcosms. Indeed, very few sequences closely related to known Fe (III) or sulfur-reducers were found in the Day 90 no added electron donor controls (Fig. S8), demonstrating that acetate amendment was required to stimulate these groups in the laterite sediment microcosms.

Some of the most frequently detected sequences in the Day 90 acetate-amended microcosms were also observed to substantially increase in relative abundance in the no added electron donor controls (Fig. S9, Table S3). All these sequences initially comprised less than 0.3 % of the Day 0 communities, indicating that they must have grown

**Table 2**
Easily recoverable metals in the Natural History Museum laterite samples (sum of aqueous and acetic-acid extractable fractions).

| | Acoje | Çaldağ | Shevchenko |
|---|---|---|---|
| **Cobalt %** | | | |
| Laterite as supplied | 0.78 ± 0.08 | 0.29 ± 0.09 | 0.07 ± 0.01 |
| No electron donor control | 3.0 | 11 | 0.63 |
| Biostimulated with acetate | 45 ± 6 | 29 ± 7 | 31 ± 2 |
| Bioaugmented with *G. sulfurreducens* + acetate | 38 ± 3 | 36 ± 5 | 30 ± 5 |
| **Nickel %** | | | |
| Laterite as supplied | 1.3 ± 0.1 | 1.3 ± 0.1 | 0.70 ± 0.05 |
| No electron donor control | 1.7 | 3.2 | 1.4 |
| Biostimulated with acetate | 10 ± 1 | 9 ± 1 | 11 ± 1 |
| Bioaugmented with *G. sulfurreducens* + acetate | 8.6 ± 0.7 | 9 ± 1 | 10 ± 1 |
| **Manganese %** | | | |
| Laterite as supplied | 0.51 ± 0.04 | 1.2 ± 0.2 | 1.3 ± 0.1 |
| No electron donor control | 2.4 | 19 | 5.5 |
| Biostimulated with acetate | 39 ± 4 | 68 ± 10 | 56 ± 6 |
| Bioaugmented with *G. sulfurreducens* + acetate | 43 ± 5 | 66 ± 9 | 62 ± 5 |
| **Iron %** | | | |
| Laterite as supplied | 0.00 ± 0.00 | 0.00 ± 0.00 | 0.00 ± 0.00 |
| No electron donor control | 0.03 | 0.03 | 0.02 |
| Biostimulated with acetate | 0.24 ± 0.07 | 5.9 ± 0.1 | 0.08 ± 0.01 |
| Bioaugmented with *G. sulfurreducens* + acetate | 1.7 ± 0.03 | 4.8 ± 0.5 | 1.6 ± 0.2 |

during the course of the 90 day experiment, whether or not acetate was added. In the Acoje and Çaldağ sediment microcosms these were primarily from the Burkholderiales and most closely related to *Herbaspirillum* spp., *Cupriavidus* spp. or assigned to the Comamonadaceae; these bacteria were previously found to be associated with sediments with redox boundaries and are known denitrifiers that can couple nitrate reduction to Fe(II) and Mn(II) oxidation. Interestingly, some species of *Herbaspirillum* and *Cupriavidus* spp. are facultative autotrophs (Ding and Yokota, 2004; Pohlmann et al., 2006) and some can fix nitrogen (Kirchhof et al., 2001; da Silva et al., 2012). The *Herbaspirillum* and *Cupriavidus* genera have been identified as a common contaminant of DNA extraction kit reagents and laboratory environments (Salter et al., 2014), but this is considered to be unlikely here due to the very low concentrations detected in the Day 0 samples (Table S3). In the Shevchenko sediment microcosms sequences most closely related to *Pseudomonas stutzeri*, another known denitrifier, were present in both the acetate-amended and the no electron donor control microcosms. Given these increases in sequences closely related to known denitrifiers it is noteworthy that the anaerobic modified freshwater minimal medium used for these sediment microcosms did not contain any added nitrate. Aqueous nitrate was not detected in the Çaldağ or the Shevchenko microcosms (Figs. S2, S3), but it was observed in the Acoje no added electron donor microcosm (Fig. 1). Together this suggests that incubation in sediment microcosms caused changes to the microbial community, particularly in groups associated with N cycling. Given that no source of organics was added, this might be linked to autotrophic growth or the metabolism of sediment organic carbon (Table S1). Either way, it is important that this effect is taken into account when interpreting shifts in microbial community composition in future sediment microcosm experiments.

The fungal community was sequenced in the acetate-amended microcosms and no electron donor controls for the Acoje laterite, to observe how the fungal community changes in sediment microcosms, and the impact of anoxic conditions caused by acetate biostimulation of sediment microbial communities. Relatively few fungal OTUs were present compared to prokaryotes (Table S2). Like the prokaryotic community there were considerable differences between the day 0 microbial community in the acetate-amended microcosm and the no electron donor control (Fig. 3D) likely due to sediment heterogeneity. The five most frequently detected fungal OTUs were typically saprotrophs and/or plant pathogens, or had no close "Type Strain" relatives (Table S4). Sequences most closely related to *Trichoderma, Alternaria,*

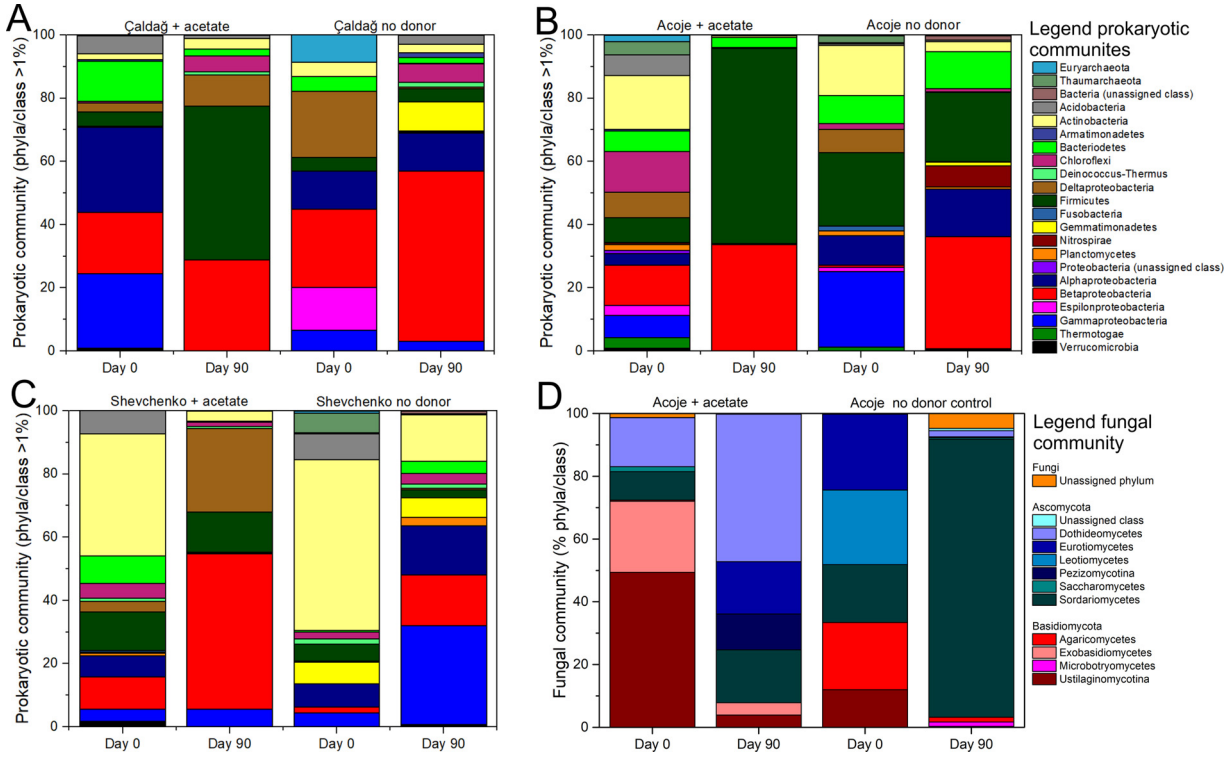


**Fig. 3.** Microbial phylogenetic diversity of the Natural History Museum laterite sediment microcosms stimulated with acetate compared to the no added electron donor controls for prokaryotes (A) Çaldağ (B) Acoje (C) Shevchenko and for fungi (D) Acoje.

*Penicillium* and *Staphylotrichum* species had increased substantially 90 days after acetate amendment, while *Purpureocillium, Pseudallescheria* and *Fusarium* species increased in the no electron donor control. These fungi are all commonly found in soil environments or associated with plants. Interestingly, *Penicillium* spp. have previously been shown to produce organic acids that could successfully bioleach Co and Ni from laterites (Tzeferis et al., 1994; Valix et al., 2001).

#### 3.2.4. Summary of microbial metal reduction in NHM laterite microcosms

Metal-reducing conditions were stimulated in the Natural History Museum laterite sediment microcosms by adding acetate, or acetate and *Geobacter sulfurreducens*, leading to Mn(IV), Fe(III) and in some cases, sulfate reduction. Although this did not cause the liberation of Co and Ni to the aqueous phase, sequential extractions showed that the amount of easily recoverable Co increased from < 1 % to up to 45 % (closely mirroring Mn behaviour) and Ni from < 1.5 % to up to 11 %. Sequencing of the prokaryotic community showed that the addition of acetate stimulated the growth of indigenous bacteria closely related to known nitrate, Mn(IV)/Fe(III) and sulfate/thiosulfate-reducers from the Clostridiales, *Anaeromyxobacter, Desulfurispora, Thermincola* and *Azoarcus* spp.

### 3.3. Piauí laterite microcosms

Samples of the Piauí laterite were biostimulated with glucose to develop metal-reducing conditions, observe the impact on Co and Ni extractability, and to identify the indigenous prokaryotes likely responsible.

#### 3.3.1. Stimulated microbial metal reduction in the Piauí laterite sediment microcosms

Given the lack of metal mobilisation to the aqueous phase observed in the acetate biostimulated NHM laterites, additional electron donors were selected to stimulate the development of metal-reducing conditions in the Piauí laterite. These included an acetate/lactate mix and glucose, which were chosen for their potential to chelate metals, and also for the potential for glucose to generate acidity during microbial metabolism. Results of initial tests showed that glucose was more effective in stimulating the indigenous microbial community to develop Mn(IV)- and Fe(III)-reducing conditions compared to a mix of acetate and lactate, and also liberated Co and Ni to the aqueous phase (Fig. S10). Therefore glucose was selected as the preferred electron donor for the Piauí laterite biostimulation experiments.

Results for sample 'Piauí 23' are shown in Fig. 4, and similar results were obtained for Piauí 4 (Fig. S11). Fe(III) reduction as monitored by the Ferrozine assay only occurred in one of the three Piauí 23 replicates (causing large error bars in the average iron(II) % values Fig. 4), and two of the three Piauí 4 replicates, therefore additional microcosms were set up to repeat the analysis for the Piauí 23 laterite (Fig. S12). In total, Fe(II) was produced in two of the five Piauí 23 microcosms but not in the other three, demonstrating considerable heterogeneity in the ability of glucose fermentation to stimulate Fe(III) reduction within this laterite sample. The pH decreased from around 8.0 to 6.5 in Piauí 23 and 6.0 in Piauí 4, and the Eh decreased slightly compared to the no electron donor control in Piauí 4.

Cobalt, manganese and nickel were released to solution in each of the glucose-biostimulated Piauí 4 and Piauí 23 microcosms but not in the no added electron donor controls, indicating that microbial processes were responsible for this metal solubilisation (Figs. 4, S11). This is in contrast to the acetate-biostimulated NHM laterites, in which limited Co, Mn and Ni were released to the aqueous phase during microbial metal reduction (Figs. 1, S2, S3). A similarly close relationship between Co and Mn geochemistry was previously observed in a bioleaching study of laterites (Smith et al., 2017).

Approximately 0.4 mM nitrate was released to the aqueous phase from the sediment in the Piauí 23 microcosms, but not in the Piauí 4 microcosms where the initial concentrations of 0.3 mM were from the added artificial groundwater (Figs. 4, S11). In both cases nitrate concentrations decreased over time likely due to microbial nitrate reduction. Unlike in the NHM laterites, no sulfate was released to the aqueous phase, and the concentration remained constant over the experiment (at ~ 0.4 mM which was added in the artificial groundwater), indicating that microbial sulfate reduction was not stimulated by glucose addition in these systems.

The microbial fermentation of glucose led to the production of volatile fatty acids (VFAs) lactate, acetate and formate. Interestingly the three Piauí 23 microcosms which did not produce Fe(II) had considerably higher VFA concentrations (5.1, 5.3, 7.6 mM), compared to the two in which Fe(II) was generated (2.6 and 3.6 mM). Given that Mn release occurred in all microcosms, likely as Mn(II) following microbial Mn(IV) reduction, it seems that in some cases the microbial community progressed through the classic terminal electron accepting processes of reducing nitrate, then Mn(IV), then Fe(III), and then towards the start of sulfate reduction (observed in one replicate, Fig. S12), while in other cases the microbial community switched towards the breakdown of glucose to generate volatile fatty acids (via fermentation). This trend was not observed in Piauí 4, where the replicate with no Fe(III) reduction had 8.5 mM total VFAs compared to the two where Fe(II) was generated which had 8.8 and 13.2 mM total VFAs. It is likely that these differences are due to heterogeneities in particular aliquots of sediment, and also across the laterite deposit, which may have implications for resource processing. The replicate Piauí 23 samples were additionally monitored at Day 264, at which point no VFAs were detected.

#### 3.3.2. Sequential extractions to investigate metal fate in the Piauí laterite sediment microcosms

To investigate the distribution of metals in the solid phase, sequential extractions were performed on the laterite as supplied and on samples of the sediment microcosms 143 days after biostimulation with glucose. Similar results were obtained for both the Piauí samples (Figs. 5, S13), showing that biostimulation of the sediment microbial communities with glucose transformed a significant proportion of metals into the acetic acid-extractable "exchangeable phase", broadly comparable to the results for the NHM laterites.

The proportion of Co associated with easily recoverable phases in the laterites (that is, the aqueous content plus the acetic-acid extractable "exchangeable" fraction) after biostimulation with glucose increased from < 0.5 % to up to 64 % while Ni increased from < 5 % to up to 12 % (Table 3). Easily recoverable Mn also increased from < 0.5 % to up to 72 %, while easily recoverable Fe increased from 0 % to up to 9 %. Far more Fe was transformed into an easily recoverable phase in the Piauí 4 sample compared to the Piauí 23 sample; additional data would be required to fully characterise this heterogeneity within the deposit prior to designing a laterite processing strategy.

#### 3.3.3. Changes to the Piauí microbial community during glucose biostimulation

Given the heterogeneity in Fe(III) reduction observed in the geochemical data, the prokaryotic microbial community was characterised in two of the Piauí 23 glucose-stimulated sediment microcosms ('Sample A' where Fe(II) was generated and partial sulfate reduction observed, and 'Sample B' where no Fe(II) was generated) and an associated no electron donor control. It was not possible to successfully extract DNA from the original biostimulation experiment shown in Fig. 4, but after optimising the DNA extraction protocols by increasing the amount of bead beating, sufficient DNA was extracted from the replicate biostimulation experiment shown in Fig. S12 at the 0, 28 and 76 day time points. Overall, relatively few prokaryotic OTUs were found in the Piauí laterite sediment microcosms (Table S2, Fig. S14) and the Shannon diversities were lower than in the NHM laterites (Table S2). This may reflect the difficulties in extracting DNA from these challenging iron oxide-rich samples. The abundance of 16S rRNA

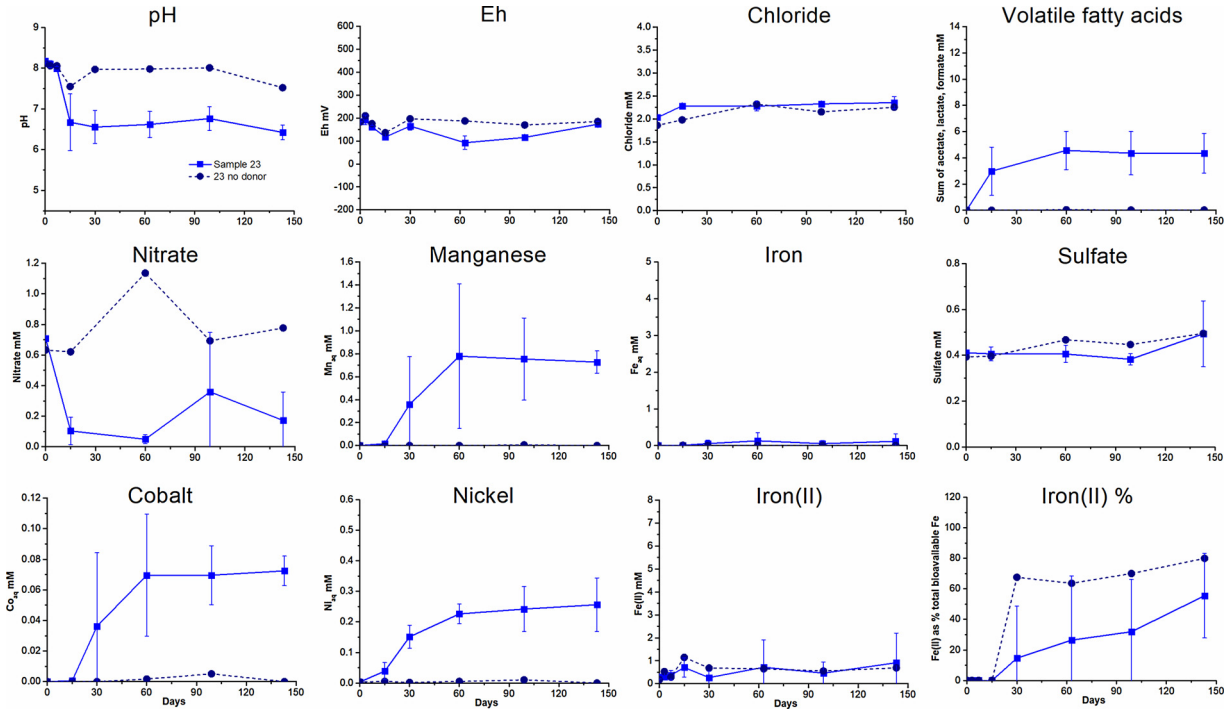


**Fig. 4.** Geochemical monitoring of the Piauí '23' laterite sediment microcosm that was biostimulated with glucose. Results are the average of three values; error bars ± 1 standard deviation. ND refers to the single no added electron donor controls (dashed lines). Data for the replicate experiment is presented in Fig. S10.

genes detected in the Day 0 samples was slightly higher than in the NHM laterites (32 – 49 fg $g^{-1}$ sediment, Table S2), but again considerably lower than the values previously reported for the Cuban laterites by Perez et al. (2013) (copy number per gram dry sample $6.6 \times 10^4$ - $1 \times 10^5$ here, compared to $1 \times 10^7$ - $1 \times 10^8$). Similar to the results for the Acoje laterite, the abundance of 16S rRNA genes detected increased over the course of the experiment in both the glucose biostimulated microcosm (from 49 to 2940 fg $g^{-1}$ laterite), and in the no added electron donor control (from 32 to 110 fg $g^{-1}$ laterite), showing incubation in sediment microcosms increased the amount of DNA, and that glucose biostimulation caused significant growth of prokaryotes. At the phylum/class level the Day 0 communities in both of the glucose-stimulated microcosms were dominated by Firmicutes (Fig. 6A) in particular, sequences most closely related to *Paenibacillus* spp., as well as Actinobacteria, Cyanobacteria and Alphaproteobacteria. The no added electron donor control contained far fewer Firmicutes.

At the OTU level the response of the two glucose stimulated microcosms was somewhat different. The composition of the microbial community in Sample A was broadly similar at Day 28 and Day 76, and dominated by sequences most closely related to *Bacillus soli* and *Paenibacillus* spp., which together made up 83 % of the prokaryotic community at Day 76 (Table S5). Both *Bacillus* and *Paenibacillus* spp. are Gram positive spore-forming facultative anaerobes typically associated with soils and the rhizosphere. *Paenibacillus* spp. are known Mn(IV) and Fe(III)-reducers (Petrie et al., 2003; Rowe et al., 2017), and the dominant OTU in Sample A was most closely related to an Fe(III)-reducing isolate from Brazilian and Cameroonian soil (Loyaux-Lawniczak et al., 2019) (Table S5). *Bacillus soli* is a facultative anaerobic capable of nitrate reduction (Heyrman et al., 2004). Neither the *Paenibacillus* nor the *Bacillus* OTUs were present in the Day 76 no added electron donor control. Although some sulfate reduction appeared to occur in Sample A (Fig. S12), few sequences closely related to known sulfate-reducers (0.01 % *Desulfitobacterium* spp.) were identified in the microbial community.

In contrast to Sample A, the Day 76 results for Sample B showed the proportion of sequences most closely related to *Bacillus* spp. decreased from 55 % to 18 % and *Paenibacillus* spp. from 19 % to 3 %, while those most closely related to *Desulfitobacterium* spp. increased from less than 0.1 % to 61 % (Table S5). *Desulfitobacterium*spp. are strict anaerobes that can use a wide range of electron acceptors including nitrate, metals, humic acids and sulfate (Villemur et al., 2006; Zhang et al., 2016). The dominant OTU in Sample B was most closely related to *Desulfitobacterium metallireducens* which is known to reduce Mn(IV), Fe(III) and thiosulfate, as well as fermenting pyruvate, but it is not able to reduce nitrate or sulfate (Villemur et al., 2006). This is interesting given that limited iron(III) reduction and increased VFA production were observed in this sample, and suggests that *Desulfitobacterium* spp. may have primarily employed a fermentative metabolism in this sample. *Desulfitobacterium* spp. were not present in the Day 76 no added electron donor control.

Like for the NHM laterites, the Day 76 control microcosm contained some similar OTUs to the biostimulated microcosms, in this case most closely related to *Porphyrobacter*, *Flavobacterium*, and *Herbaspirillum* spp. from freshwater environments, the rhizosphere, and from studies of phototrophy and cyanobacteria associations (Table S5). However, most of these were also present in the Day 0 Piauí microcosms, suggesting that they remained present throughout the course of the experiment rather than their growth being stimulated by incubation in sediment microcosms.

Relatively few fungal OTUs were detected during the Piauí 23 microcosm experiment (Table S2). The five most frequently detected fungal OTUs were typically saprotrophs and/or plant pathogens, or had no close Type Strain relatives (Table S6). It appeared that glucose biostimulation favoured the growth of fungi closely related to *Fusarium* spp., which made up more than 80 % of the day 28 and day 76 glucose-amended microcosms (Fig. 6B). Sequences most closely related to *Alternaria, Penicillium* and *Talaromyces* species increased over time in the no electron donor control. Interestingly, *Alternaria* and *Penicillium* species were found to be stimulated by acetate amendment in the Acoje laterite (Table S4), but given the low quantity of total organic carbon (0.05 %) in the Piauí laterite their increase in proportion in the Piauí control is unexplained. Again, the potential for *Penicillium* spp. to bioleach Co and Ni from laterites has previously been demonstrated (Tzeferis et al., 1994; Valix et al., 2001).

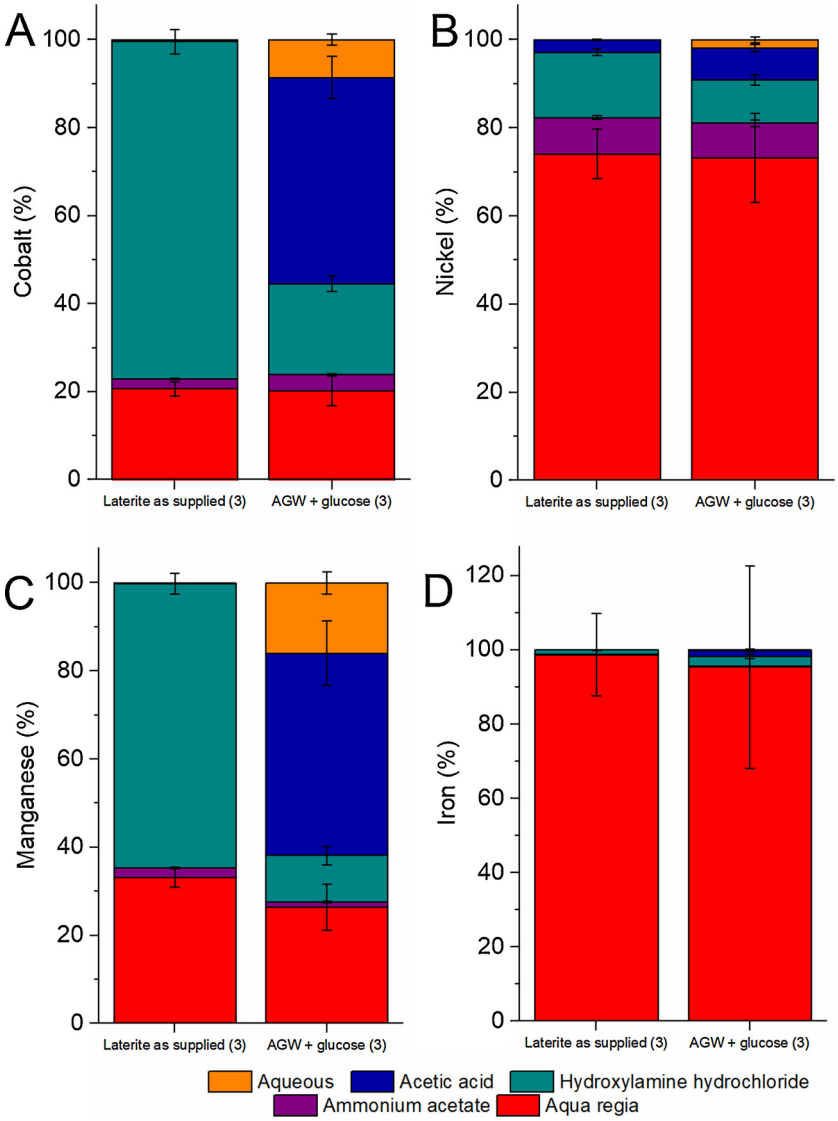


**Fig. 5.** Analysis of metal distribution in the Piauí 23 laterite using sequential extractions (A) cobalt (B) nickel (C) manganese (D) iron. The laterite as supplied (left hand column) showed very little metals in the acetic-acid extractable "exchangeable" phase. Biostimulation of the sediment microbial community with glucose (right hand column) increased the proportion of Co, Mn and Ni associated with the acetic-acid extractable "exchangeable" phase. Numbers in brackets represent the number of replicates used for the sequential extraction procedure.

**Table 3**
Easily recoverable metals in the Piauí laterites samples (sum of aqueous and acetic-acid extractable fractions).

| | Piauí 4 | Piauí 23 |
|---|---|---|
| **Cobalt %** | | |
| Laterite as supplied | 0.36 ± 0.02 | 0.43 ± 0.02 |
| Biostimulated with glucose | 64 ± 3 | 56 ± 5 |
| **Nickel %** | | |
| Laterite as supplied | 4.9 ± 0.4 | 2.8 ± 0.2 |
| Biostimulated with glucose | 12 ± 1 | 9 ± 1 |
| **Manganese %** | | |
| Laterite as supplied | 0.25 ± 0.03 | 0.19 ± 0.01 |
| Biostimulated with glucose | 72 ± 7 | 62 ± 8 |
| **Iron %** | | |
| Laterite as supplied | 0.00 ± 0.00 | 0.00 ± 0.00 |
| Biostimulated with glucose | 9 ± 2 | 1.7 ± 0.4 |

*3.3.4. Summary of microbial metal reduction in Piauí laterite microcosms*

Metal-reducing conditions were stimulated in the Piauí laterite sediment microcosms by adding glucose, which led to Mn(IV) reduction and liberation of Co and Ni. Sequential extractions showed that the amount of easily recoverable Co increased from < 0.5 % to up to 64 % (closely mirroring Mn behaviour) and Ni from < 5 % to up to 12 %. Fe (III) reduction was observed in two of the five Piauí 23 replicates, demonstrating heterogeneity in the sediment, which was also reflected in the composition of the prokaryotic communities. Known Mn(IV)/Fe (III)-reducers (e.g. *Paenibacillus*) were initially present in all of the samples. In Sample A the proportion of *Paenibacillus* remained high at Day 76 (unlike in the no electron donor control), suggesting it might have been responsible for metal reduction, but in Sample B glucose biostimulation appeared to promote fermentative metabolisms which generated an increased quantity of VFAs rather than Fe(II).

*3.4. Solid phase characterisation in the laterites before and after incubation in sediment microcosms*

A range of different techniques were applied to characterise the laterites as supplied and after incubation in sediment microcosms, and to observe the impact of the development of microbial metal-reducing

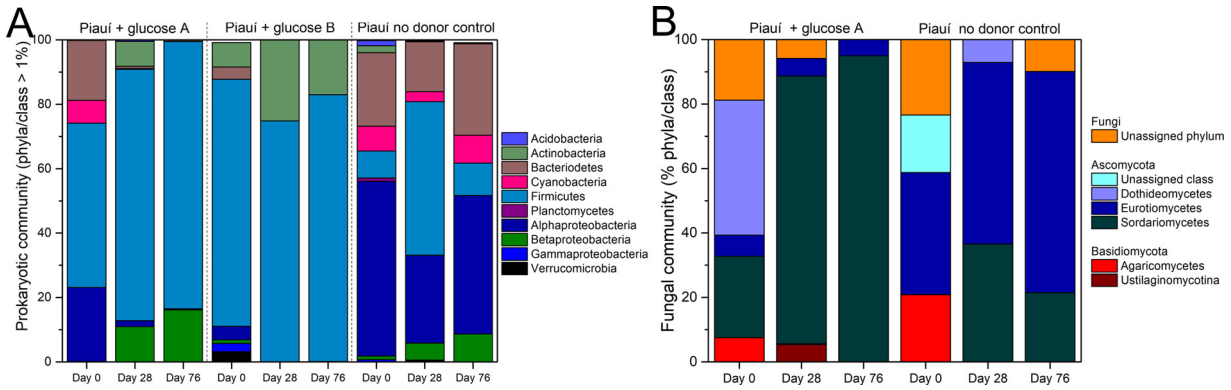


**Fig. 6.** Microbial phylogenetic diversity of the Piauí laterite sediment microcosms stimulated with glucose compared to the no added electron donor controls, (A) prokaryotic community), (B) fungal community.

conditions on the laterite mineralogy and metal speciation.

### 3.4.1. XRD

Changes in mineralogy in the laterites before and after the development of reducing conditions were examined using XRD. Goethite was present in the XRD patterns of all the laterites at the start and end of the experiment. Mn oxides were not apparent in the XRD patterns, but this was not surprising given the Mn content of the laterites was < 1 % (dry weight). For the most part where haematite, clinochlore and hornblende were identified in the XRD patterns in the laterites as supplied, they were absent from the corresponding biostimulated and bioaugmented sediment microcosms, suggesting the development of microbial metal-reducing conditions caused them to decrease below the level of detection by XRD, that is, less than 5 % by mass (Fig. S16). Maghemite was observed in all the biostimulated and bioaugmented samples, but its absence in the Acoje and Çaldağ laterites as supplied suggests it may have formed during the development of reducing conditions. Kaolinite was only observed in the biostimulated and bioaugmented Piauí 23 and Shevchenko sediment microcosms, and siderite was only observed in the bioaugmented Acoje sediment microcosm. Overall this indicates that the development of reducing conditions in sediment microcosms principally affected the Fe-bearing minerals haematite, clinochlore and hornblende. Maghemite, kaolinite and siderite appeared post-reduction, while goethite remained present throughout the experiment.

### 3.4.2. X-ray absorption spectroscopy

Samples were analysed by XAS to determine the speciation of Co, Ni, Fe and Mn before and after biostimulation. Fe and Ni concentrations were sufficiently high to obtain $L_{II}$ and $L_{III}$ edge XAS, while concentrations of Co and Mn were too low for this technique. Additional beam time allowed *K*-edge XAS to be collected for Co and Ni, with the concentrations of Ni sufficiently high to collect EXAFS data.

*3.4.2.1. Iron speciation.* The iron $L_{II}$ and $L_{III}$ edge XAS were very similar for the laterites as supplied, and after incubation in biostimulated sediment microcosms (Fig. 7A). No significant XMCD signal was measurable from any of the samples. Comparing the spectra with the known Fe(III) standards ferrihydrite, goethite and hematite and the mixed Fe(II)/Fe(II) standard magnetite (Joshi et al., 2018) showed the samples had the same spectral shape as the pure Fe(III) standards, particularly at the diagnostic $L_3$ edge. In addition, the trough between the two positive peaks of the $L_3$ edge was greater in the samples than in the ferrihydrite standard and more similar in size to goethite (hematite was not considered to be as relevant as goethite was identified to be present by XRD).

*3.4.2.2. Nickel speciation.* Nickel speciation was determined using both $L_{II}$ and $L_{III}$ edges and *K*-edge XAS. Nickel $L_{II}$ and $L_{III}$ edge spectra could only be obtained for the Çaldağ and the Piauí laterites, despite the Çaldağ laterite having the lowest Ni content. The spectra for both laterites closely resembled a known calculated standard for Ni(II) in octahedral coordination (Fig. 7B) (Laan and Kirkman, 1992; Coker et al., 2008). Ni *K*-edge XANES spectra were also similar for all samples, both before and after biostimulation (Fig. 8A) and indicative of Ni in octahedral coordination in goethite; the position of the main peak (~8349 eV) was close to published values for Ni in goethite (Landers et al., 2011), and the presence of a small pre-edge feature at 8333 eV indicated that Ni was in octahedral coordination with minimal distortion (Landers et al., 2011).

Three models were tested to fit the Ni *K*-edge EXAFS informed by the literature on Ni speciation in other laterites; Ni in Mg-phyllosilicates (Roqué-Rosell et al., 2017), Ni in goethite (Manceau et al., 2000; Landers et al., 2011) and Ni in Mn-oxides (Roqué-Rosell et al., 2010). The best fitting parameters were obtained for Ni in goethite (Fig. 8B, Table S7), with 6 Ni-O at 2.05 Å, 2.6–3.9 Ni-Fe at 3.07 Å (edge-sharing) and 1.5–5.5 Ni-Fe at 3.49 Å (corner-sharing). These values closely reflected published values (Manceau et al., 2000; Landers et al., 2011) and Ni substituted in goethite corresponds with the high Fe contents measured by XRF, and the presence of goethite in the XRD patterns (Table S1). Differences in the coordination numbers fitted for Ni-Fe between the laterites suggests substitution of Ni into different positions in the goethite crystal lattice. Although reasonable fitting parameters were obtained for Ni in Mn-oxides, this model had 6 Mn atoms surrounding Ni which was not considered physically-realistic given the laterites contained 1.5–4.4 times more Ni than Mn (Table S7). Ni in Mg-phyllosilicates had significantly worse fitting parameters.

*3.4.2.3. Cobalt speciation.* The Co *K*-edge XANES spectra for the laterites as supplied mostly closely resembled the Co-doped $MnO_2$ standard (Fig. 9), and the position of the main peak (7730 eV) was similar to reported values for Co(III)OOH (Dublet et al., 2017). Although under most environmental conditions Co(II) is thermodynamically favoured, in the presence of Mn(IV)-oxides it has been shown to sorb and rapidly (within 12 h) oxidise to Co(III) (Tanaka et al., 2013; Simanova and Peña, 2015). Cobalt(III) bearing Mn(III/IV)-oxides are also known to form during weathering of laterites (Dublet et al., 2017). The XANES spectra for the Çaldağ and Shevchenko laterites as supplied show a broader peak profile around 4–5 eV in width spanning the range of values for Co(II) and Co(III), and suggesting that they contained a mixture of Co(II) and Co(III). Similar profiles were observed for less-weathered laterites found at depth and interpreted as containing Co present in olivine and serpentinite (Dublet et al., 2017). Post-reduction, the main Co peak shifted towards lower energies in each laterite (Fig. 9, Table S8), indicating reduction of Co (III) to Co(II), which has a main absorption edge at 7725 eV (Dublet et al., 2017).

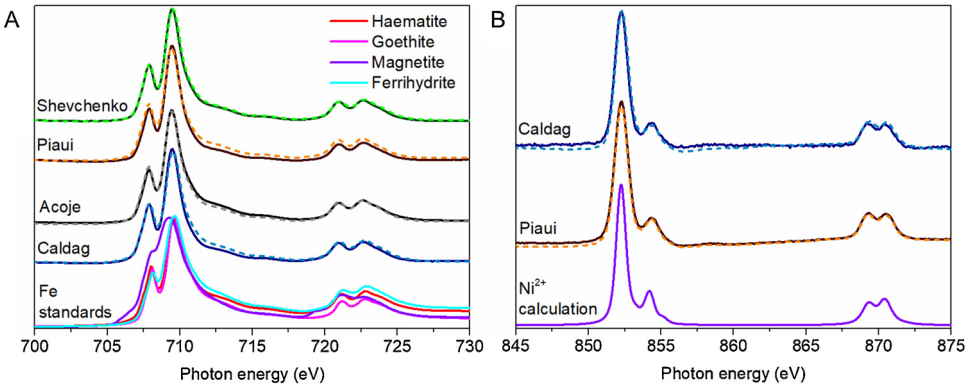


**Fig. 7.** $L_{II}$ and $L_{III}$ edge spectra for (A) Fe (and B) Ni for the laterites as supplied (solid lines) and at the end of the sediment microcosm study (dashed lines) compared to standards; metal speciation appeared the same in the laterites as supplied and in the microbially reduced sediments.

*3.4.3. Summary of the impact of microbial metal reduction on laterite mineralogy*

All four laterites were dominated by goethite, both before and after incubation in sediment microcosms. It appeared that microbial Fe(III) reduction did not occur substantially in these experiments, with iron predominantly present as Fe(III) both before and after incubation in sediment microcosms (Figs. 7, S16). Most of the signal from *L*-edge XAS occurs from the surface 3–4 nm of a sample (Byrne et al., 2013), and therefore any reduced Fe(II)-containing minerals ought to have been identifiable using this technique. Previous work showed both XRD patterns and TEM images for immature and crystalline goethite were similar before and after incubation with *G. sulfurreducens*, suggesting goethite is relatively recalcitrant to microbial Fe(III) reduction (Cutting et al., 2009). Moreover, the sequential extraction data showed that 97–99 % of Fe in the laterites as supplied was present in the aqua regia extractable "residual" phase (Figs. 2,5, S5, S6) and therefore was unlikely to be bioavailable. Although small increases in the acetic-acid extractable "exchangeable" phase were observed in the laterites after incubation in sediment microcosms, and the proportion of Fe(II) increased during the course of the experiment (Figs. 1,4, S1, S2), overall the mineralogy remained dominated by the large quantities of goethite present.

The Ni $L_{II}$ and $L_{III}$ edge and *K* edge XAS spectra for each laterite were very similar before and after the development of metal-reducing conditions (Figs. 7 and 8), demonstrating that (in the solid phase) Ni remained in association with the microbiologically-recalcitrant goethite throughout the course of the experiment. The sequential extraction data showed the proportion of Ni associated with the "exchangeable" acetic-acid extractable fraction increased from around 1 % (Table 2) or 5 % (Table 3) to around 10 % (Tables 2,3). This could be due to the liberation of Ni from Mn(IV)-oxides, which have previously been identified in laterites (Roqué-Rosell et al., 2010), but in these samples they would have formed a very small proportion of the sample and therefore did not make a significant contribution to the EXAFS spectra. Nonetheless, these results suggest that stimulating the development of reducing conditions in laterites is likely to have a small but beneficial effect on the recovery of Ni.

The Co *K* edge XAS spectra showed that it was initially present as Co (III), likely incorporated into Mn-oxide minerals that formed < 1.5 % (w/w) of the laterites (Fig. 9). After reducing conditions were stimulated by the addition of an organic substrate, Co was shown to be reduced to Co(II) or a mixed Co(II)/Co(III) phase. This corresponds with the sequential extraction data that showed a significant proportion of Co was transformed from a hydroxylamine hydrochloride extractable "reducible" form to an acetic acid extractable "exchangeable" phase, considered to represent the sorbed fraction (Figs. 2,5, S5, S6, S13). The mechanism by which this occurred during the development of reducing conditions in sediment microcosms is likely to be linked to the microbial reduction of Mn(IV) oxides to Mn(II), releasing Co(III) from the crystal structure, which then sorbs back to the laterite as Co(II) (Tanaka et al., 2013). It was not possible to infer from this dataset whether Co (III) was reduced to Co(II) as a result of thermodynamic equilibration upon dissolution of Mn-oxides via microbial Mn(IV) reduction, or whether direct microbial reduction of Co(III) had occurred (previously observed by Gorby et al., 1998).

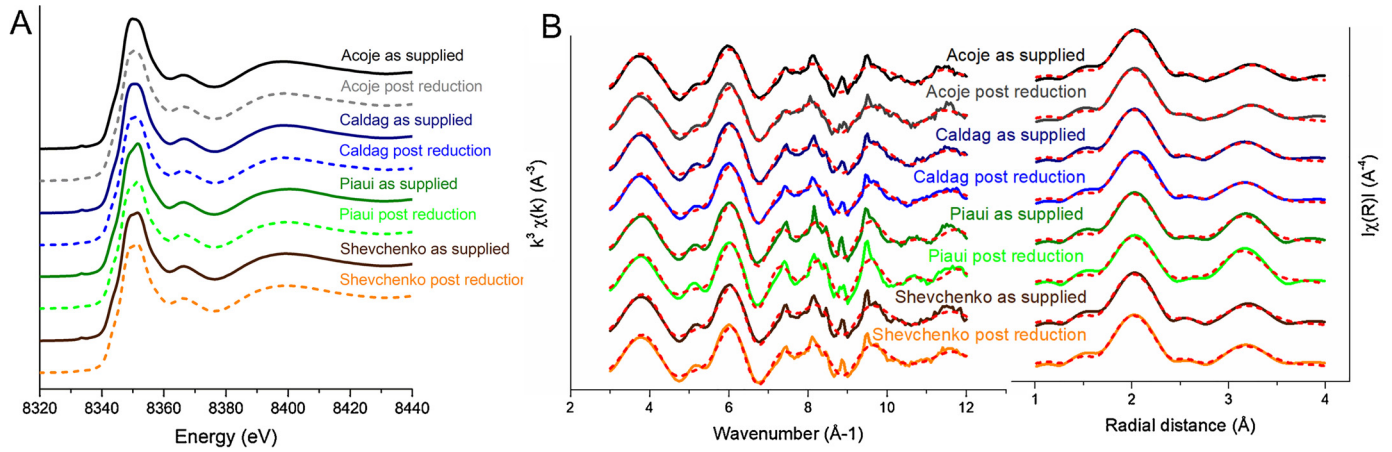


**Fig. 8.** Ni *K*-edge XAS spectra (A) XANES and (B), EXAFS and Fourier transform of EXAFS for the laterites as supplied (solid lines) and at the end of the sediment microcosm study (dashed lines for XANES, solid lines for EXAFS). Best fits for the EXAFS are shown as red dashed lines and were obtained for Ni substituted in goethite.

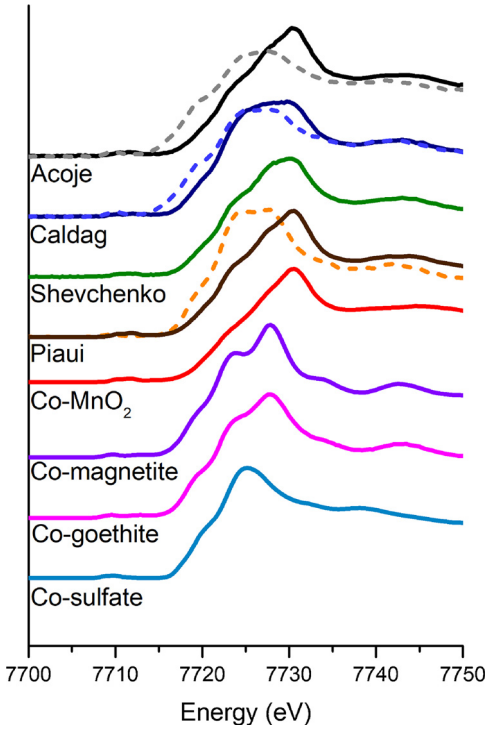


**Fig. 9.** Co *K*-edge XANES of laterites as supplied (solid lines) and at the end of the sediment microcosm study (dashed lines) compared to standards. The peak of Co-doped $MnO_2$ at 7730 eV represents Co(III) and Co-sulfate at 7725 eV represents Co(II), similar to the standards reported in Dublet et al. (2017). Co speciation in the doped magnetite and goethite standards is similar, and resembles the Co-serpentinite and Co-olivine reported in Dublet et al. (2017). The post-reduction Shevchenko sample was not analysed.

### *3.5. Implications for Co and Mn biogeochemical cycling*

Co and Mn concentrations were positively correlated in the laterites (Fig. S1) and Co was likely present as Co(III) incorporated into Mn oxides (Fig. 9). This corresponds with previous data showing Co being associated with Mn-oxide enriched horizons in laterites (Elias et al., 1981; Yongue-Fouateu et al., 2006; Dublet et al., 2017), and in soil environments (Taylor and McKenzie, 1966; Uren, 2013).

Here we stimulated the natural microbial community in the laterites to develop metal-reducing conditions by adding acetate or glucose. The results showed very similar geochemical behaviour for Co and Mn; neither metal was released to solution in the acetate biostimulated NHM laterites (Figs. 1, S2, S3), while in the glucose biostimulated Piauí laterite the time series plots showed that Co and Mn were released to the aqueous phase at remarkably similar rates, indicating a close association and that the mechanism of Co release was likely to be microbial Mn(IV) reduction (Fig. 4). The distributions of Co and Mn in the laterites observed using sequential extractions were again very comparable (Figs. 2,5, S5, S6) both before and after microbial metal reduction. Together, these results show that redox cycling plays a dynamic and defining role in controlling the fate of Co and Mn in these sediment systems.

### *3.6. Applying microbial metal reduction to bioprocess laterites*

Biostimulation of laterites with acetate or glucose dramatically increased the proportion of easily recoverable Co (and to a lesser extent Ni), without transforming the majority of the iron oxides. Therefore a new two-step bioprocessing strategy to recover Co (and some Ni) from laterite ores is proposed. First, the laterites should be treated with organic substrates such as glucose or acetate (or potentially similar simple sources of cheaply available or waste carbon) and left for a period of time to allow metal-reducing conditions to develop, after which they should be rinsed with acetic acid. This will mobilise up to 64 % of the Co, with minimal dissolution of Fe. Different organic substrates may stimulate respirative or fermentative metabolisms; which although both capable of mobilising Co, should be taken into account when assessing their cost-effectiveness. It appears that glucose biostimulation may be a more promising for use in a laterite processing technique compared to acetate biostimulation as it generated both aqueous and "exchangeable" Co and Ni, and extracted a higher proportion of metals from the laterite.

The results presented here showed that up to 64 % of the Co present in these laterites could be recovered by this process. Further benefits are gained from the minimal amount of Fe-based crystalline minerals mobilised during the process, which will negate the need to separate Fe from the processed product, and lessen the requirement for dealing with large quantities of associated iron oxide wastes. Additional work would be required to assess the suitability of this two-step laterite treatment process in an industrial scenario, including cost-benefit analyses and feasibility studies, but these are beyond the scope of the current study. Experiments to investigate whether Co is mobilised under flowing conditions that more closely represent how this technology might be deployed in an industrial scenario in an industrial scenario are ongoing.

## 4. Conclusions

Microbial metal reduction was stimulated in laterites using organic substrates. Large quantities of Co (and smaller amounts of Ni) were transformed from a 'reducible' phase to a more labile 'exchangeable' phase, which was leachable using acetic acid. The organic substrates stimulated the growth of indigenous metal-reducing prokaryotes which were likely responsible for Mn(IV) reduction and Co mobilisation. Increases in the proportion of fungi that produce beneficial organic acids previously shown to leach Co and Ni were observed, and this could also have played a role in metal solubilisation. These results are compelling given that similar behaviour observed in four laterites (Acoje, Çaldağ, Piauí and Shevchenko) from different continents. In addition to generating new data on how the solubility of Co is controlled during microbial redox cycling in lateritic soils, this also informs a new two-step bioprocessing strategy that is proposed to recover Co from laterites.

The results presented here demonstrate that Co can be biogeochemically cycled in sediments. Co and Mn association has previously been observed in many different environments, and here Co behaviour was closely linked to that of Mn, suggesting Co mobility will consequently be controlled by Mn(IV)-reducing and Mn(II)-oxidising bacteria. These groups are ubiquitous in sediments, and indeed were observed to be present in each of the four laterites analysed. This highlights the important role of microbial processes in the weathering of laterites, and their contribution to the enrichment of Co within Mn oxide minerals.

## 5. Funding

This work was supported by the Natural Environment Research Council (CoG3 NE/M011518/1). Beamtime at beamline I20 was funded by grants SP16735 and SP17313 from Diamond Light Source. This research used resources of the Advanced Light Source, which is a DOE Office of Science User Facility under contract no. DE-AC02-05CH11231.

## Declaration of Competing Interest

The authors declare that they have no known competing financial interests or personal relationships that could have appeared to influence the work reported in this paper.

## Acknowledgements

We are very grateful to Paul Lythgoe, Alastair Bewsher, John Waters, Heath Bagshaw and Roseanna Byrne (University of Manchester) for analytical support with ICP-AES, ion chromatography, XRF, TOC, XRD, TEM and qPCR. We thank Sulaiman Mulroy (University of Manchester) for collecting the Co XANES spectra at Diamond Light Source and providing the Co-MnO2 standard, and Sandra Dressler (Loughborough University) for providing the Co-goethite standard. We thank Shusaku Hayama (I20, Diamond Light Source) and Alpha N'Diaye (6.3.1, Advanced Light Source) for their advice on how to use their beamlines. We would additionally like to thank Mike and Ann Oxley (Brazilian Nickel) for allowing LN to collect samples from the Piauí deposit, and the Natural History Museum for access to their sample collection.

## Appendix A. Supplementary data

Supplementary material related to this article can be found, in the online version, at doi:https://doi.org/10.1016/j.chemgeo.2019.119330.

## References

Bacon, J.R., Davidson, C.M., 2008. Is there a future for sequential chemical extraction? Analyst 133, 25–46.
British Geological Survey, 2009. Cobalt. British Geological Survey, Keyworth, Nottingham.
Brown, A.E., Muthumeenakshi, S., Sreenivasaprasad, S., Mills, P.R., Swinburne, T.R., 1993. A PCR primer-specific to *Cylindrocarpon heteronema* for detection of the pathogen in apple wood. FEMS Microbiol. Lett. 108, 117–120.
Byrne, J.M., Coker, V.S., Moise, S., Wincott, P.L., Vaughan, D.J., Tuna, F., Arenholz, E., Van Der Laan, G., Pattrick, R.A.D., Lloyd, J.R., Telling, N.D., 2013. Controlled cobalt doping in biogenic magnetite nanoparticles. J. R. Soc. Interface 10, 20130134.
Caporaso, J.G., Kuczynski, J., Stombaugh, J., Bittinger, K., Bushman, F.D., Costello, E.K., Fierer, N., Peña, A.G., Goodrich, J.K., Gordon, J.I., Huttley, G.A., Kelley, S.T., Knights, D., Koenig, J.E., Ley, R.E., Lozupone, C.A., McDonald, D., Muegge, B.D., Pirrung, M., Reeder, J., Sevinsky, J.R., Turnbaugh, P.J., Walters, W.A., Widmann, J., Yatsunenko, T., Zaneveld, J., Knight, R., 2010. QIIME allows analysis of high-throughput community sequencing data. Nat. Methods 7, 335–336.
Caporaso, J.G., Lauber, C.L., Walters, W.A., Berg-Lyons, D., Huntley, J., Fierer, N., Owens, S.M., Betley, J., Fraser, L., Bauer, M., Gormley, N., Gilbert, J.A., Smith, G., Knight, R., 2012. Ultra-high-throughput microbial community analysis on the Illumina HiSeq and MiSeq platforms. ISME J. 6, 1621–1624.
Caporaso, J.G., Lauber, C.L., Walters, W.A., Berg-Lyons, D., Lozupone, C.A., Turnbaugh, P.J., Fierer, N., Knight, R., 2011. Global patterns of 16S rRNA diversity at a depth of millions of sequences per sample. Proc. Natl. Acad. Sci. U.S.A. 108, 4516–4522.
Chen, G., Yang, H., Li, H., Tong, L., 2016. Recovery of cobalt as cobalt oxalate from cobalt tailings using moderately thermophilic bioleaching technology and selective sequential extraction. Minerals 6, 67.
Coker, V.S., Bell, A.M.T., Pearce, C.I., Pattrick, R.A.D., van der Laan, G., Lloyd, J.R., 2008. Time-resolved synchrotron powder X-ray diffraction study of magnetite formation by the Fe(III)-reducing bacterium *Geobacter sulfurreducens*. Am. Mineral. 93, 540–547.
Crowe, S.A., O'Neill, A.H., Weisener, C.G., Kulczycki, E., Fowle, D.A., Roberts, J.A., 2007. Reductive dissolution of trace metals from sediments. Geomicrobiol. J. 24, 157–165.
Cutting, R.S.S., Coker, V.S.S., Fellowes, J.W.W., Lloyd, J.R.R., Vaughan, D.J.J., 2009. Mineralogical and morphological constraints on the reduction of Fe(III) minerals by *Geobacter sulfurreducens*. Geochim. Cosmochim. Acta 73, 4004–4022.
Ding, L., Yokota, A., 2004. Proposals of *Curvibacter gracilis* gen. nov., sp. Nov. And *Herbaspirillum putei* sp. Nov. For bacterial strains isolated from well water and reclassification of [*Pseudomonas*] *huttiensis*, [*Pseudomonas*] *lanceolata*, [*Aquaspirillum*] *delicatum* and [*Aquaspirillum*] *autotrophicum* as *Herbaspirillum huttiense* comb. nov., *Curvibacter lanceolatus* comb. nov., *Curvibacter delicatus* comb. Nov. And *Herbaspirillum autotrophicum* comb. Nov. Int. J. Syst. Evol. Microbiol. 54, 2223–2230.
Downward, L., Booth, C.H., Lukens, W.W., Bridges, F., 2007. A variation of the F-Test for determining statistical relevance of particular parameters in EXAFS fits. AIP Conf. Proc. 882, 129–131.
Dublet, G., Juillot, F., Brest, J., Noël, V., Fritsch, E., Proux, O., Olivi, L., Ploquin, F., Morin, G., 2017. Vertical changes of the Co and Mn speciation along a lateritic regolith developed on peridotites (New Caledonia). Geochim. Cosmochim. Acta 217, 1–15.
Edgar, R.C., 2010. Search and clustering orders of magnitude faster than BLAST. Bioinformatics 26, 2460–2461.
Edgar, R.C., 2013. UPARSE: highly accurate OTU sequences from microbial amplicon reads. Nat. Methods 10, 996–998.
Edgar, R.C., Haas, B.J., Clemente, J.C., Quince, C., Knight, R., 2011. UCHIME improves sensitivity and speed of chimera detection. Bioinformatics 27, 2194–2200.
Elias, M., Donaldson, M.J., Giorgetta, N., 1981. Geology, mineralogy and chemistry of lateritic nickel-cobalt deposits near Kalgoorlie, Western Australia. Econ. Geol. 76, 1775–1783.
European Commission, 2011. Tackling the Challenges in Commodity Markets and on Raw Materials. Brussels.
Gardes, M., Bruns, T.D., 1993. ITS primers with enhanced specificity for basidiomycetes–application to the identification of mycorrhizae and rusts. Mol. Ecol. 2, 113–118.
Gorby, Y.A., Caccavo, F.J., Bolton, H.J., 1998. Microbial reduction of cobalt$^{III}$EDTA$^{-}$ in the presence and absence of manganese(IV) oxide. Environ. Sci. Technol. 32, 244–250.
Gweon, H.S., Oliver, A., Taylor, J., Booth, T., Gibbs, M., Read, D.S., Griffiths, R.I., Schonrogge, K., 2015. PIPITS: an automated pipeline for analyses of fungal internal transcribed spacer sequences from the Illumina sequencing platform. Methods Ecol. Evol. 6, 973–980.
Haas, B.J., Gevers, D., Earl, A.M., Feldgarden, M., Ward, D.V., Giannoukos, G., Ciulla, D., Tabbaa, D., Highlander, S.K., Sodergren, E., Methé, B., DeSantis, T.Z., Human Microbiome Consortium, T.H.M., Petrosino, J.F., Knight, R., Birren, B.W., 2011. Chimeric 16S rRNA sequence formation and detection in Sanger and 454-pyrosequenced PCR amplicons. Genome Res. 21, 494–504.
Hayama, S., Duller, G., Sutter, J.P., Amboage, M., Boada, R., Freeman, A., Keenan, L., Nutter, B., Cahill, L., Leicester, P., Kemp, B., Rubies, N., Diaz-Moreno, S., 2018. The scanning four-bounce monochromator for beamline I20 at the Diamond Light Source. J. Synchrotron Radiat. 25, 1556–1564.
Hem, J.D., 1985. Study and Interpretation of the Chemical Characteristics of Natural Water. US Geological Survey, Alexandria, VA.. .
Heyrman, J., Vanparys, B., Logan, N.A., Balcaen, A., Rodríguez-Díaz, M., Felske, A., De, V.P., 2004. *Bacillus novalis* sp. nov., *Bacillus vireti* sp. nov., *Bacillus soli*sp. nov.,*Bacillus bataviensis* sp. nov. and *Bacillus drentensis* sp. nov., from the Drentse A grasslands. Int. J. Syst. Evol. Microbiol. 54, 47–57.
Johnson, D., Grail, B., Hallberg, K., Johnson, D.B., Grail, B.M., Hallberg, K.B., 2013. A new direction for biomining: extraction of metals by reductive dissolution of oxidized ores. Minerals 3, 49–58.
Joshi, N.A., Fass, J.N., 2011. Sickle: a Sliding-window, Adaptive, Quality-based Trimming Tool for FastQ Files [Software]. Available at. http://github.com/najoshi/sickle.
Joshi, N., Filip, J., Coker, V.S., Sadhukhan, J., Safarik, I., Bagshaw, H., Lloyd, J.R., 2018. Microbial reduction of natural Fe(III) minerals; toward the sustainable production of functional magnetic nanoparticles. Front. Environ. Sci. 6, 127.
Keith-Roach, M.J., Morris, K., Dahlgaard, H., 2003. An investigation into technetium binding in sediments. Mar. Chem. 81, 149–162.
Kirchhof, G., Eckert, B., Stoffels, M., Ivo Baldani, J., Reis, V.M., Hartmann, A., 2001. *Herbaspirillum frisingense* sp. nov., a new nitrogan-fixing bacterial species that occurs in C4-fibre plants. Int. J. Syst. Evol. Microbiol. 51, 157–168.
Kozich, J.J., Westcott, S.L., Baxter, N.T., Highlander, S.K., Schloss, P.D., 2013. Development of a dual-index sequencing strategy and curation pipeline for analyzing amplicon sequence data on the MiSeq Illumina sequencing platform. Appl. Environ. Microbiol. 79, 5112–5120.
Kursunoglu, S., Kaya, M., 2016. Atmospheric pressure acid leaching of Caldag lateritic nickel ore. Int. J. Miner. Process. 150, 1–8.
van der, Laan G., Kirkman, I.W., 1992. The 2p absorption spectra of 3d transition metal compounds in tetrahedral and octahedral symmetry. J. Phys. Condens. Matter 4, 4189–4204.
Landers, M., Gräfe, M., Gilkes, R.J., Saunders, M., Wells, M.A., 2011. Nickel distribution and speciation in rapidly dehydroxylated goethite in oxide-type lateritic nickel ores: XAS and TEM spectroscopic (EELS and EFTEM) investigation. Australian J. Earth Sci. 58, 745–765.
Lane, D.J., 1991. 16S/23S rRNA sequencing. In: Stackebrant, E., Goodfellow, M. (Eds.), Nucleic Acid Techniques in Bacterial Systematics. John Wiley & Sons Ltd, London, pp. 115–175.
Lovley, D.R., Holmes, D.E., Nevin, K.P., 2004. Dissimilatory Fe(III) and Mn(IV) reduction. In: Poole, R.K. (Ed.), Advances in Microbial Physiology. Academic Press, pp. 219–286.
Lovley, D.R., Phillips, E.J., 1986. Organic matter mineralization with reduction of ferric iron in anaerobic sediments. Appl. Environ. Microbiol. 51, 683–689.
Lovley, D.R., Phillips, E.J.P., 1988. Novel mode of microbial energy metabolism: organic carbon oxidation coupled to dissimilatory reduction of iron or manganese. Appl. Environ. Microbiol. 54, 1472–1480.
Lovley, D.R., Phillips, E.J.P., 1987. Rapid assay for microbially reducible ferric iron in aquatic sediments. Appl. Environ. Microbiol. 53, 1536–1540.
Lovley, D.R., Phillips, E.J.P., Gorby, Y.A., Landa, E.R., 1991. Microbial reduction of uranium. Nature 350, 413–416.
Loyaux-Lawniczak, S., Vuilleumier, S., Geoffroy, V.A., 2019. Efficient reduction of iron oxides by *Paenibacillus* spp. strains isolated from tropical soils. Geomicrobiol. J. 1–10.
Manceau, A., Schlegel, M., Musso, M., Sole, V., Gauthier, C., Petit, P., Trolard, F., 2000. Crystal chemistry of trace elements in natural and synthetic goethite. Geochim. Cosmochim. Acta 64, 3643–3661.
Marrero, J., Coto, O., Goldmann, S., Graupner, T., Schippers, A., 2015. Recovery of nickel and cobalt from laterite tailings by reductive dissolution under aerobic conditions using *Acidithiobacillus* species. Environ. Sci. Technol. 49, 6674–6682.
Marsh, E., Anderson, E., Gray, F., 2013. Nickel-cobalt Laterites - a Deposit Model. In Mineral Deposit Models for Resource Assessment. Scientific Investigations Report 2010-5070-H. US Geological Survey, Reston, Virginia. .
Martin, M., 2011. Cutadapt removes adapter sequences from high-throughput sequencing reads. EMBnet.journal 17, 10.
Masella, A.P., Bartram, A.K., Truszkowski, J.M., Brown, D.G., Neufeld, J.D., 2012. PANDAseq: paired-end assembler for Illumina sequences. BMC Bioinformatics 13, 31.
Murray, J.W., Dillard, J.G., 1979. The oxidation of cobalt(II) adsorbed on manganese dioxide. Geochim. Cosmochim. Acta 43, 781–787.

Myers, C.R., Nealson, K.H., 1988. Bacterial manganese reduction and growth with manganese oxide as the sole electron acceptor. Science (80-.) 240, 1319–1321.
Nurk, S., Bankevich, A., Antipov, D., Gurevich, A.A., Korobeynikov, A., Lapidus, A., Prjibelski, A.D., Pyshkin, A., Sirotkin, A., Sirotkin, Y., Stepanauskas, R., Clingenpeel, S.R., Woyke, T., Mclean, J.S., Lasken, R., Tesler, G., Alekseyev, M.A., Pevzner, P.A., 2013. Assembling single-cell genomes and mini-metagenomes from chimeric MDA products. J. Comput. Biol. 20, 714–737.
Oxley, A., Smith, M.E., Caceres, O., 2016. Why heap leach nickel laterites? Miner. Eng. 88, 53–60.
Pattrick, R.A.D., Van Der Laan, G., Henderson, C.M.B., Kuiper, P., Dudzik, E., Vaughan, D.J., 2002. Cation site occupancy in spinel ferrites studied by X-ray magnetic circular dichroism: developing a method for mineralogists. Eur. J. Mineral. 14, 1095–1102.
Perez, O.C., Coto, J.M., Schippers, A., 2013. Quantification of the microbial community in lateritic deposits. Integr. Sci. Ind. Knowl. Biohydrometall. 825, 33–36.
Petrie, L., North, N.N., Dollhopf, S.L., Balkwill, D.L., Kostka, J.E., 2003. Enumeration and characterization of iron(III)-reducing microbial communities from acidic subsurface sediments contaminated with uranium(VI). Appl. Environ. Microbiol. 69, 7467–7479.
Pohlmann, A., Fricke, W.F., Reinecke, F., Kusian, B., Liesegang, H., Cramm, R., Eitinger, T., Ewering, C., Pötter, M., Schwartz, E., Strittmatter, A., Voß, I., Gottschalk, G., Steinbüchel, A., Friedrich, B., Bowien, B., 2006. Genome sequence of the bioplastic-producing "Knallgas" bacterium *Ralstonia eutropha* H16. Nat. Biotechnol. 24, 1257–1262.
Rauret, G., López-Sánchez, J.F., Sahuquillo, A., Rubio, R., Davidson, C., Ure, A., Quevauviller, P., F. Lopez-Sanchez, J., 1999. Improvement of the BCR three step sequential extraction procedure prior to the certification of new sediment and soil reference materials. J. Environ. Monit. 1, 57–61.
Ravel, B., Newville, M., 2005. ATHENA, ARTEMIS, HEPHAESTUS: data analysis for X-ray absorption spectroscopy using IFEFFIT. J. Synchrotron Radiat. 12, 537–541.
Reinhold-Hurek, B., Hurek, T., 2006. The genera *Azoarcus, Azovibrio, Azospira* and *Azonexus*. *The Prokaryotes*. Springer New York, New York, NY, pp. 873–891.
Roqué-Rosell, J., Mosselmans, J.F.W., Proenza, J.A., Labrador, M., Galí, S., Atkinson, K.D., Quinn, P.D., 2010. Sorption of Ni by "lithiophorite-asbolane" intermediates in Moa Bay lateritic deposits, eastern Cuba. Chem. Geol. 275, 9–18.
Roqué-Rosell, J., Villanova-de-Benavent, C., Proenza, J.A., 2017. The accumulation of Ni in serpentines and garnierites from the Falcondo Ni-laterite deposit (Dominican Republic) elucidated by means of μXAS. Geochim. Cosmochim. Acta 198, 48–69.
Rowe, A.R., Yoshimura, M., LaRowe, D.E., Bird, L.J., Amend, J.P., Hashimoto, K., Nealson, K.H., Okamoto, A., 2017. *In situ* electrochemical enrichment and isolation of a magnetite-reducing bacterium from a high pH serpentinizing spring. Environ. Microbiol. 19, 2272–2285.
Salter, S.J., Cox, M.J., Turek, E.M., Calus, S.T., Cookson, W.O., Moffatt, M.F., Turner, P., Parkhill, J., Loman, N.J., Walker, A.W., 2014. Reagent and laboratory contamination can critically impact sequence-based microbiome analyses. BMC Biol. 12, 87.
Shaheen, S.M., Rinklebe, J., Frohne, T., White, J.R., DeLaune, R.D., 2014. Biogeochemical factors governing cobalt, nickel, selenium, and vanadium dynamics in periodically flooded Egyptian North Nile Delta rice soils. Soil Sci. Soc. Am. J. 78, 1065.
da Silva, K., Florentino, L.A., da Silva, K.B., de Brandt, E., Vandamme, P., de Souza Moreira, F.M., 2012. *Cupriavidus necator* isolates are able to fix nitrogen in symbiosis with different legume species. Syst. Appl. Microbiol. 35, 175–182.
Simanova, A.A., Peña, J., 2015. Time-resolved investigation of cobalt oxidation by Mn (III)-rich δ-$MnO_2$ using quick X-ray absorption spectroscopy. Environ. Sci. Technol. 49, 10867–10876.
Singh, R., Dong, H., Liu, D., Marts, A.R., Tierney, D.L., Almquist, C.B., 2015. [Cobalt (III)–EDTA] − reduction by thermophilic methanogen *Methanothermobacter thermautotrophicus*. Chem. Geol. 411, 49–56.
Slack, J.F., Kimball, B.E., Shedd, K.B., 2017. In: Schulz, K.J., DeYoung, J.H.J., Seal, R.R.I., Bradley, D.C. (Eds.), Cobalt. In Critical Mineral Resources of the United States—Economic and Environmental Geology and Prospects for Future Supply: U.S. Geological Survey Professional Paper 1802, pp. F1–F40 Reston, Virginia.
Smith, S.L., Grail, B.M., Johnson, D.B., 2017. Reductive bioprocessing of cobalt-bearing limonitic laterites. Miner. Eng. 106, 86–90.
Tanaka, K., Yu, Q., Sasaki, K., Ohnuki, T., 2013. Cobalt(II) oxidation by biogenic Mn oxide produced by *Pseudomonas* sp. strain NGY-1. Geomicrobiol. J. 30, 874–885.
Taylor, D.L., Walters, W.A., Lennon, N.J., Bochicchio, J., Krohn, A., Caporaso, J.G., Pennanen, T., 2016. Accurate estimation of fungal diversity and abundance through improved lineage-specific primers optimized for Illumina amplicon sequencing. Appl. Environ. Microbiol. 82, 7217–7226.
Taylor, R., McKenzie, R., 1966. The association of trace elements with manganese minerals in Australian soils. Aust. J. Soil Res. 4, 29.
The Cobalt Institute, 2019. The Cobalt Institute. Webpage. Available at: https://www.cobaltinstitute.org/ (Accessed January 22, 2019). .
Tzeferis, P.G., Agatzini, S., Nerantzis, E.T., 1994. Mineral leaching of non-sulphide nickel ores using heterotrophic micro-organisms. Lett. Appl. Microbiol. 18, 209–213.
Uren, N., 2013. Cobalt and manganese. In: Alloway, B.J. (Ed.), Heavy Metals in Soils: Trace Metals and Metalloids in Soils and Their Bioavailability. Springer, Netherlands, pp. 335–366.
US Geological Survey, 2018. Mineral Commodity Summaries: Cobalt. US Geological Survey, Reston, Virginia. .
Valix, M., Usai, F., Malik, R., 2001. Fungal bio-leaching of low grade laterite ores. Miner. Eng. 14, 197–203.
Villemur, R., Lanthier, M., Beaudet, R., Lépine, F., 2006. The *Desulfitobacterium* genus. FEMS Microbiol. Rev. 30, 706–733.
Vos, P., Garrity, G.M., Jones, D., Krieg, N.R., Ludwig, W., Rainey, F.A., Schleifer, K.-H., Whitman, W.B., 2009. Bergey's Manual of Systematic Bacteriology, 2nd ed. The Firmicutes 3 Springer, Dordrecht Heidelberg London New York.
Wang, Q., Garrity, G.M., Tiedje, J.M., Cole, J.R., 2007. Naive Bayesian classifier for rapid assignment of rRNA sequences into the new bacterial taxonomy. Appl. Environ. Microbiol. 73, 5261–5267.
Wilkins, M.J., Livens, F.R., Vaughan, D.J., Beadle, I., Lloyd, J.R., 2007. The influence of microbial redox cycling on radionuclide mobility in the subsurface at a low-level radioactive waste storage site. Geobiology 5, 293–301.
Yongue-Fouateu, R., Ghogomu, R.T., Penaye, J., Ekodeck, G.E., Stendal, H., Colin, F., 2006. Nickel and cobalt distribution in the laterites of the Lomié region, south-east Cameroon. J. Afr. Earth Sci. 45, 33–47.
Zavarzina, D.G., Sokolova, T.G., Tourova, T.P., Chernyh, N.A., Kostrikina, N.A., Bonch-Osmolovskaya, E.A., 2007. *Thermincola ferriacetica* sp. nov., a new anaerobic, thermophilic, facultatively chemolithoautotrophic bacterium capable of dissimilatory Fe (III) reduction. Extremophiles 11, 1–7.
Zhang, X., Li, G.-X., Chen, S.-C., Jia, X.-Y., Wu, K., Cao, C.-L., Bao, P., 2016. Draft genome sequence of *Desulfitobacterium hafniense* strain DH, a sulfate-reducing bacterium isolated from paddy soils. Genome Announc. 4, e01693–15.